Student thesis series INES nr 637

Modelling the impact of climate change on future carbon dynamics of northern peatlands

Agnes Pierre

2024
Department of
Physical Geography and Ecosystem Science
Lund University
Sölvegatan 12
S-223 62 Lund
Sweden

Agnes Pierre (2024).

Modelling the impact of climate change on future carbon dynamics of northern peatlands

Master degree thesis, 30 credits in *Physical Geography and Ecosystem Science*
Department of Physical Geography and Ecosystem Science, Lund University

Level: Master of Science (MSc)

Course duration: *August* 2024 until *January* 2024

Disclaimer

Modelling the impact of climate change on future carbon dynamics of northern peatlands

---

Agnes Pierre

Master thesis, 30 credits, in *Physical Geography and Ecosystem Science*

Wenxin Zhang
Lund University

Nitin Chaudhary
Lund University

Exam committee:
Paul Miller, Lund University
Alexandra Pongrácz, Lund University

Abstract

Northern peatlands, spanning across vast regions of the northern hemisphere, are critical carbon reservoirs essential for global carbon cycling and climate regulation. Their dual role as long-term atmospheric carbon dioxide (CO_2) sinks and the largest natural source of methane (CH_4) in the northern hemisphere allows them to accumulate more carbon than they emit, helping to mitigate the rise in atmospheric CO_2 levels. However, they face significant threats from ongoing climate change, while the local response to climate change is divided. The potential impacts of increasing temperatures, altered precipitation patterns and shifts in hydrology have the capacity to accelerate decomposition rates and release stored carbon into the atmosphere, thereby exacerbating global warming. Conversely, the net productivity of peatland ecosystems also increases due to CO_2 fertilization and prolonged growing seasons in northern latitudes. This study employs the dynamic global vegetation model LPJ-GUESS to analyse historical and future carbon dynamics of northern peatlands, aiming to reduce uncertainty surrounding peatland carbon stocks by evaluating the historical model results and assessing the fate of four northern peatlands under CMIP5 projections (RCP2.6 and RCP8.5). The project does not only identify the temporal and spatial patterns of the peatland carbon stocks and greenhouse gas emissions at these sites but also quantify how these patterns are in response to climatic drivers.

Evaluation against available datasets and literature reveals underestimations in modelled annual carbon sink capacities) and overestimated CH_4 emissions, introducing uncertainties in future carbon balance assessments. Despite limitations, the trend in future carbon stocks suggests a potential reduction across Canadian sites under RCP8.5, while the sites demonstrate resilience under RCP2.6. The high emissions scenario (RCP8.5) projects Stordalen and Mer Bleue to potentially transition into carbon sources by 2100, while NEP trends in Scotty Creek and Attawapiskat indicate robust carbon sink capacities, with varying methane emissions driven by changing hydrology and vegetation shifts. These findings underscore the complex interplay of climate, vegetation composition, and permafrost thawing in shaping future peatland carbon dynamics. Despite model underestimations of carbon sink capacities, the observed trends in net ecosystem productivity (NEP) offer valuable insights into potential future trajectories. Future research should prioritize refining model inputs and incorporating bias-corrected historical data to enhance simulation accuracy and deepen our understanding of peatland responses to climate change.

Table of Contents

1. Introduction

1.1 Introduction

Peatlands constitute 30% of the global soil organic carbon pool, making them one of the largest terrestrial carbon pools globally (Yu et al., 2009, Qiu et al., 2022). Northern peatlands (latitude 40° to 70°N) extend over 3.2 million km^2 and store between 400-600 Pg C and have the capacity to significantly impact the global carbon cycle and the climate (Loisel et al., 2014; 2016; Qiu et al., 2022; Yu, 2010; 2012). The dynamics of peatland ecosystems play a significant role in the global carbon cycle due to their dual role as long-term atmospheric carbon dioxide (CO_2) sinks and as the largest natural source of methane (CH_4) in the northern hemisphere (Yu et al., 2009, Zhang et al., 2017). Contemporary approximations of CH_4 emissions from northern peatlands lie between 10-36 Tg CH_4 y^{-1} (Abdalla et al., 2016; Loisel et al., 2016). However, their capacity to accumulate more carbon than they emit leads to a net accumulation of carbon, which helps mitigate the rise in atmospheric CO_2 levels (Loisel et al., 2014). As carbon sinks, peatlands sequester carbon through photosynthesis and slow decomposition rates as result of the environmental conditions of peatlands. The ongoing global warming, however, poses a significant threat to the current peatland carbon stock. The potential impacts of increasing temperatures, altered precipitation patterns and shifts in hydrology have the capacity to accelerate decomposition rates and release stored carbon into the atmosphere, thereby exacerbating global warming. Conversely, the net productivity of peatland ecosystems also increases due to CO_2 fertilization and prolonged growing seasons in northern latitudes (Loisel et al., 2016).

Approximately 40% of northern peatlands are underlain by permafrost, which influences peat accumulation by reducing plant productivity and decomposition (Loisel et al., 2016; Qui et al., 2022). Due to recent global warming, permafrost thawing has exposed previously stored carbon for decomposition and changed the hydrological conditions by raising water tables. This process, in turn, disrupts carbon dynamics by promoting heightened microbial respiration and CH_4 emissions as anaerobic soil conditions increase. Understanding the carbon dynamics of peatland ecosystems from a historical and future perspective is essential, especially as high-latitude ecosystems such as the Arctic have been warming nearly four times faster than to the global average (Rantanen et al., 2022).

Only a limited number of dynamic global vegetation models (DGVMs) have integrated peatland ecosystems into their framework for the purpose of simulating historical peat accumulation and projecting ecosystem responses to future climate conditions. Among these models, LPJ-GUESS, a process-based DGVM, stands out for its inclusion of peatland dynamics (Chaudhary et al. 2017a). However, uncertainty still surrounds how northern peatland carbon dynamics will respond to climate change. Existing research efforts have mainly focused on regional-scale modelling, typically using a limited selection of climate projection scenarios to represent one high and one low-emission scenario. However, there is a pressing need for more localised simulations that encompass the full range of climate scenarios available within a given climate projection framework (Chaudhary et al., 2022; Qiu et al., 2022). As northern peatland ecosystems profoundly impact the global carbon dynamics and climate regulation in the light of global warming, it is of high importance that our understanding of the future of these ecosystems evolve (Loisel et al., 2021).

1.2 Aims and objectives

The aim of this study is to assess the effects of future projected climate on northern peatland carbon dynamics. The overall purpose of the study is to assess the uncertainty surrounding peatland carbon stocks by implementing and evaluating the peatland-vegetation model LPJ-GUESS on various sites under hindcast and future climate (Chaudhary et al. 2017a, 2020). The project will not only identify temporal and spatial patterns of the peatland carbon stocks and greenhouse gas emissions at these sites but also quantify how these patterns are in response to future climatic drivers.

1.3 Research questions

To what extent does the LPJ-GUESS model accurately depict historical peatland dynamics at the designated study sites when contrasted with available datasets and literature?

What are the anticipated changes in peatland carbon stocks and fluxes by 2100 based on CMIP5 climate projections?

Which sites are particularly vulnerable to shift from carbon stocks to sources in the future, and what factors contribute to this susceptibility?

2. Background

2.1 Northern peatland ecosystems

Northern peatlands started forming about 12000 years ago when ice sheets retreated after the last glacial maximum (Loisel et al., 2016). Northern peatlands encompass various subtypes such as bogs, fens, and peat plateaus and are prevalent across several regions in the mid- and high latitudes of the Northern Hemisphere (Loisel et al., 2016). Bogs are rain-fed and nutrient poor with relatively low production and decomposition rates, in contrast to fens which are connected to groundwater, thereby having higher nutrient content and subsequently higher production rates. Bogs are dominated by bryophytes such as *Sphagnum* mosses, while graminoids such as cotton grasses *Eriophorum* spp., sedges and woody vegetation also are common in fens or peatlands located in warmer climate (Finlayson & Milton, 2018; Vitt, 2008). The key regions include Continental Western Canada (CWC), the Hudson Bay Lowlands (HBL), Russian Far East (RFE), West Siberian Lowlands (WSL), and Northern Europe (NE), each contributing uniquely to the global carbon cycle (Fig. 1). While RFE and WSL are less explored peatland regions, they cover vast areas and have together with HBL been identified as crucial carbon stock hotspots that play a significant role in the global carbon cycle (Chaudhary et al., 2017b; Chaudhary et al., 2022). Canada contains a large proportion of the global peatland extent and has an estimated peatland carbon stock of ~150 Pg C, much of which HBL and CWC contribute to (Chartrand et al., 2023; Harris et al., 2021). HBL alone stores about ~30 Pg C, which represents about 25% and 6% of the Canadian and northern peatland carbon pool respectively (Helbig et al., 2019; Packalen et al., 2014). An even larger proportion of the peatland carbon stock of 214 Pg C has been estimated

in Russia, which includes the regions RFE and WSL (Yu 2012). The carbon stocks in the remaining northern peatland regions, such as Europe and USA, are estimated to be smaller (Yu, 2012).

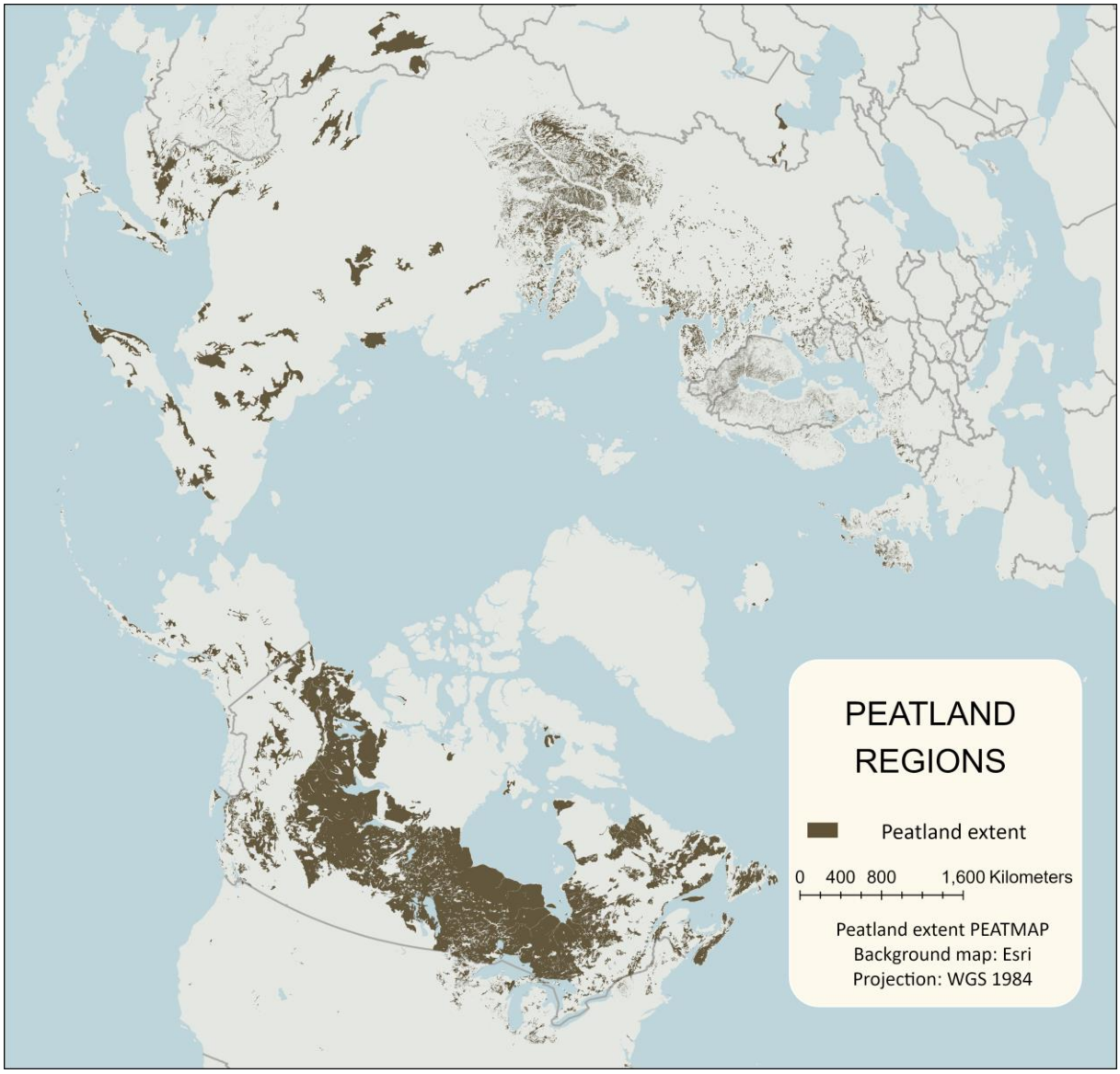

Figure 1. Sub-arctic and temperate peatland regions across the northern hemisphere with peatland extent from PEATMAP (Xu et al., 2017).

Peatlands maintain their carbon dynamics through an intricate balance of carbon accumulation and carbon losses through decomposition as CO_2 and CH_4. The core of peatland carbon dynamics is the accumulation of peat, partially decomposed plant material, due to waterlogged and anoxic conditions. As organic matter in peatlands decomposes at a slower rate than it is produced due to cold, acidic, and waterlogged conditions, carbon accumulates over thousands of years in peatlands (Loisel et al., 2016). Carbon is released from peatlands as CO_2 and CH_4 through decomposition of organic matter, where CH_4 emissions commonly occur in anaerobic and waterlogged conditions, such as the northern peatland. The release of CH_4 to the atmosphere is regulated by the production rate and transportation capacity from the soil to the atmosphere (Packalen et al., 2014). Anaerobic microorganisms, primarily archaea,

thrive in waterlogged conditions and produce CH_4 during the decomposition of organic matter. These microorganisms utilise CO_2 and hydrogen released during decomposition to generate CH_4. This CH_4 can then escape to the atmosphere through diffusion, transportation through plants, and sediment ebullition, contributing to greenhouse gas emissions (Packalen et al., 2014; Saunois et al., 2020). As CH_4 production is partly controlled by anaerobic and waterlogged conditions, temperature, and substrate availability, it increases in response to rising water tables which can occur due to seasonal variations or changing climate conditions (Saunois et al., 2016). Historically, the capacity of northern peatlands to accumulate more carbon than they release has resulted in them a persistent carbon sink with a negative radiative impact on the climate (Loisel et al., 2016, Roulet et al., 2007).

Permafrost within peatland ecosystems plays a significant role in carbon dynamics. About 40% of the northern peatlands are underlain by permafrost, and in Canada alone, about 80% of the carbon pool within peatlands is stored in permafrost (Chartrand et al., 2023; Loisel et al., 2016; Qui et al., 2022). As permafrost thaws, previously preserved organic matter becomes susceptible to decomposition and carbon is released to the atmosphere as CO_2 or CH_4. Furthermore, permafrost thaw can change the hydrological dynamics of peatlands, potentially increasing water table levels and consequently increasing CH_4 emissions. Moreover, thaw-induced subsidence of permafrost plateaus creates new wetland features such as waterlogged depressions, impacting carbon storage and CH_4 fluxes.

2.2 CMIP5 scenarios and their projected impact on peatland ecosystems

Climate scenarios from the Coupled Model Intercomparison Project phase 5 (CMIP5) are used within the climate modelling community to investigate the effects of past, present, and future climate. The climate projections and associated data infrastructure have become essential to the Intergovernmental Panel on Climate Change (IPCC) and other international or national climate assessment reports. CMIP5 is a modelling framework that combines results from different general circulation models into a single multi-model ensemble. This approach enhances the realism of results by incorporating a range of model responses to identical forcing scenarios. The Representative Concentration Pathways (RCP) scenarios are used within the CMIP5 framework to provide plausible future radiative forcing projections based on anticipated projected population growth, technical developments, energy requirements, and other socioeconomic variables (Taylor et al., 2012). They include the low emission scenario RCP2.6, the intermediate scenarios RCP4.5 and RCP6.0, and the high emission scenario RCP8.5, where each RCP scenario is named after its projective total radiative forcing in $W\ m^{-2}$ by the year 2100.

As global temperatures rise at an accelerating pace, the Arctic and subarctic regions are exposed to even higher temperature increases. Various studies indicate that the Arctic is warming at a rate of two to four times faster than the global average (Rantanen et al., 2022). This accelerated warming is expected to alter precipitation patterns and cause rapid thawing of permafrost (ICOS, n.d.; Rantanen et al., 2022). If global temperatures exceed a 1.5°C increase from pre-industrial levels, the severity of consequences stemming from peatland drying and permafrost thawing is expected to escalate (O'Neill et al., 2022). The consequences of global warming are already observed, and include increased wildfires, mass

mortality of trees, drying of peatlands, and thawing of permafrost, leading to a weakening in land carbon sinks and increased greenhouse gas emissions. As temperatures continue to rise and precipitation patterns shift, many peatlands are expected to dry out due to increased evapotranspiration and reduced precipitation, thereby decreasing their carbon sequestering capacity (Parmesan et al., 2022; IPCC, 2023). As decomposition rates increase with temperature, peatland carbon emissions are likely to increase and further amplify climate change. Permafrost currently stores vast amounts of frozen carbon, which thawed, would become available for decomposition, and increase carbon emissions to the atmosphere. The thawing of permafrost also alters the hydrology of peatlands, affecting vegetation composition and carbon dynamics within peatlands.

2.3 LPJ-GUESS peatland model

The Lund-Potsdam-Jena General Ecosystem Simulator, known as LPJ-GUESS, is a widely used dynamic global vegetation model (DGVM) in studies focusing on global carbon cycles and vegetation dynamics. LPJ-GUESS is a process-based model used to simulate vegetation dynamics, plant physiology, and biogeochemistry in terrestrial ecosystems which employs an individual- and patch-based representation of vegetation and ecosystems (Smith et al., 2001; Miller & Smith, 2012). The model can simulate both local and regional ecosystem processes and has been evaluated against independent datasets and other models (Chaudhary et al., 2017a; 2017b; Qiu et al., 2022). This project employs a customised Arctic version of LPJ-GUESS where peatland dynamics has been developed and validated, which has been used for modelling peatland carbon dynamics across the northern hemisphere (Chaudhary et al. 2017a). This customised version accounts for plant diversity and environmental factors specific to peatlands. This customised version of LPJ-GUESS was used since it is able to simulate critical peatland processes, such as peat accumulation and decomposition, and permafrost dynamics, enabling the simulation of complex hydrological, biophysical, and biogeochemical processes in Arctic and peatland ecosystems.

2.3.1 Plant functional types

Plant functional types (PFTs) specific for peatland ecosystems have also been included in the model framework to represent specific vegetation types in arctic ecosystems (Chaudhary et al., 2017a; Miller & Smith, 2012). The peatland PFTs includes mosses and lichens, graminoids, low evergreen shrubs, low and tall summer green shrubs, vegetation that thrive in both inundated and dry conditions. Each PFT has defined parameters relating to e.g., waterlogging tolerance, litter decomposability, and phenology which in turn determine their interaction with the environment. The PFTs establish within bioclimatic limits and are restricted by the annual-average WTP. Shrubs establish deeper, while mosses and graminoids thrive in wet conditions. A brief description of some of the key processes in the peatland framework is given below, while a detailed description can be found in Chaudhary et al., 2017b.

2.3.2 Carbon accumulation and decomposition

To accurately simulate soil thermal dynamics, the model incorporates a multi-layered soil-peat column where each column is divided into four vertically distinct layers (Chaudhary et al., 2017b). A dynamic snow layer covers the peat, followed by a variable litter-peat layer with sublayers that are updated annually. A two-metre-deep mineral soil column with two sublayers follows the peat, which in turn is underlain by a 48-metre-deep padding column consisting of various sublayers. In the model, peat accumulation results from carbon input exceeding decomposition, leading to carbon accumulation. The peat column is divided into two layers, the upper which experiences fluctuating water tables and allows aerobic and anaerobic litter decomposition, and the lower which is found below the water table, resulting in slow decomposition and increased peat accumulation due to the constantly waterlogged conditions (Chaudhary et al., 2017b). One type of carbon input to peatland ecosystems is the addition of litter, which each year is deposited over existing peat layers, transforming into peat due to high carbon mineralization rates. Different PFTs contribute to carbon accumulation in the litter pool at varying rates based on productivity, mortality, and leaf turnover. Decomposition rates vary among PFTs, with graminoid litter decomposing faster than shrubs, while moss litter decomposes at the slowest rate. Decomposed litter carbon is released as respiration, and the remaining mass becomes a new peat layer in the following year.

2.3.3 Hydrology and permafrost dynamics

Peatland hydrology is simulated with a water bucket scheme, where precipitation and snowmelt input water to the ecosystem, which then is removed through evapotranspiration, drainage, and runoff (Chaudhary et al., 2017a). WTP are updated on a daily time step based on the existing WTP, the daily net input of water, and porosity and permeability of the peat. WTP above 0 indicate water tables above the peat surface. The landscape WTP is updated daily, affecting the landscape's overall hydrology and indirectly vegetation composition and decomposition rates. Decomposition rates are assumed to be at high under dry soil conditions, while the lowest decomposition rates are associated with waterlogged conditions. The soil temperature at different depths is calculated on a daily time step based on the daily surface air temperature, and the temperature in the peat layers are updated subsequently (Miller & Smith, 2012). The thermal properties of the peat layers are determined by the physical properties of minerals, organic matter, and peat, as well as amount of water and ice. The process of freezing and thawing in peat and mineral soil layers impact plant dynamics, hydrology, and carbon fluxes in permafrost peatlands. Peat does not decompose under frozen soil conditions, i.e. when the fraction of ice content is larger than zero (Chaudhary et al., 2017a)

2.3.4 Net primary production and methane

Net primary production (NPP) is determined by the balance between photosynthesis and autotrophic respiration. Photosynthesis is modelled on a daily time step using a coupled photosynthesis and water module adapted from BIOME3 (Smith et al., 2001). The module provides area-based averaged for gross primary production (GPP) per PFT, which in turn is related to air temperature, atmospheric CO_2 concentrations, absorbed photosynthetically

active radiation (PAR) and stomatal conductance (Tang et al. 2015). Autotrophic respiration comprises energy-demanding processes in vegetation that results in a release of CO_2 and a reduction in NPP. CH_4 is generated as methanogens consume a potential carbon pool, and is released as a fraction of heterotrophic respiration (Wania et al., 2009a; 2009b; 2010). CH_4 can be released to the atmosphere through diffusion, plant-mediated transport, and ebullition. The net emission of methane is determined by the balance between production and oxidation. Oxidation of CH_4 is generated by methanotrophic bacteria which turn CH_4 into CO_2, a process that primarily is influenced by the water table position in the model, and peat temperature.

2.3.5 Vegetation establishment and fire disturbance

The model is able to simulate both vegetation establishment and mortality. It includes a vegetation establishment function which is implemented annually based on the mean annual WTP. The PFT establishment is determined by the tolerance to waterlogged soil conditions, in addition to other prescribed limits. While shrubs are vulnerable to waterlogged conditions and thereby only establish when mean annual WTP is deeper than -25 cm below the surface, graminoids and mosses establish in wetter soil conditions (Chaudhary et al., 2017a). Vegetation mortality is simulated through the implementation of a prognostic wildfire module, where the risk of fire events increases under dry and warm climate conditions.

2.4 Previous modelling studies on the future of northern peatlands

Existing modelling studies with LPJ-GUESS and other DGVMs have investigated potential changes in regional and global peatland carbon stocks under future climate scenarios. Studies that have modelled the near future predict that northern peatlands will remain carbon sinks by 2100 under RCP4.5 and RCP6.0, while increasing respiration rates following a warmer climate could shift some peatlands into carbon neutral under RCP8.5 (Chaudhary et al., 2022). Studies agree that peatlands in northern Europe are at risk of becoming carbon sources or carbon neutral in the future due to continued global warming, mainly caused by increasing decomposition rates in warmer soils (Chaudhary et al., 2017a; 2020; Qiu 2022). In contrast, the peatland regions in the HBL, CWC, and WSL are modelled to remain stable carbon sinks until 2100, with a potential increase in their carbon sink capacity (Chaudhary et al., 2017a; 2022). The latter has been concluded by multiple modelling studies, which have shown that northern peatlands are expected to sequester more carbon in the near future due to a projected milder and wetter climate, a longer growing season, and the CO_2 fertilisation effect (Chaudhary et al., 2017b; Loisel et al., 2016; Zhang et al., 2013). Two modelling studies have observed hot spots of increasing CH_4 emissions in the HBL, CWC, and WSL, likely driven by permafrost thaw and enhanced soil decomposition (Zhang et al., 2013; Qiu et al., 2022). Additionally, peatlands underlain by permafrost, which include vast parts of the northern peatlands, are modelled to disappear from various key regions in the coming decades due to the rapid permafrost thaw, potentially exacerbating global warming (Chaudhary et al., 2022).

An intercomparison study of five state-of the-art peatland models was performed by Qiu et al., 2022 to assess future changes in CO_2 and CH_4 fluxes across northern peatlands. The models included the LPJ-GUESS with dynamic multi-peat layers used in this project, an Arctic LPJ-GUESS version without dynamic peat layers, as well as ORCHIDEE-PEAT, LPJ-

MPI, and LPX-Bern. Two of the models, namely LPJ-GUESS and LPX-Bern, include coupled nitrogen and carbon cycling, in comparison to the other models where NPP is not limited by the availability of soil nitrogen. The study concluded that northern peatlands would remain carbon sinks until 2300 under RCP2.6, while CWC, HBL, NE, and WSL are projected to shift into carbon sources or carbon neutral under RCP8.5 (Qiu et al., 2022). Only one model, namely LPJ-GUESS with incorporated nitrogen cycling, simulated RFE as a future net carbon source by 2300, and this model version performed better at capturing interannual variability of water table positions. In this study, the two models that incorporated nitrogen cycling projected the peatlands to become greater CO_2 sources compared to the other models where NPP was not restricted by soil nitrogen. The two models which explicitly simulated coupled peatland nitrogen and carbon cycling projected that these peatlands will be larger CO_2 sources in the future, as opposed to the models in which NPP is not limited by available soil nitrogen.

3. Data and methodology

3.1 Site descriptions

The model simulations were performed on four sites across the northern peatland dominated regions (Fig. 2). The sites were strategically chosen to ensure a spatial distribution across different peatland types and climate and were based on the availability of observed data on carbon stocks and fluxes for evaluating model results. Out of these locations, Abisko-Stordalen, Scotty Creek, and Attawapiskat are located in the subarctic region where permafrost occurrence is sporadic, while the Mer Bleue site represents a temperate peatland environment with no permafrost (Table 1).

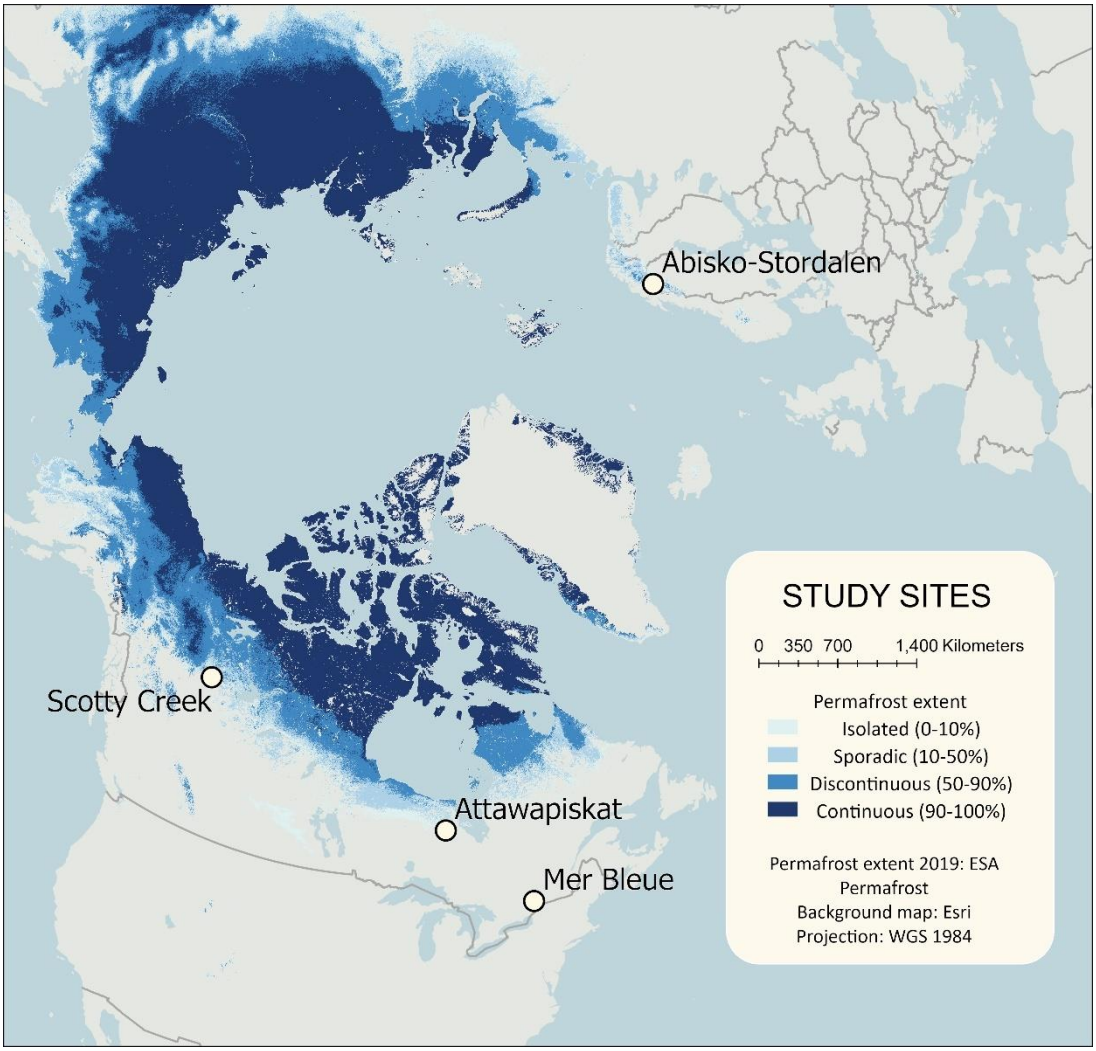

Figure 2. Study sites and permafrost extent classified as isolated, sporadic, discontinuous, or continuous. Permafrost extent year 2019 from the European Space Agency's Permafrost Climate Change Initiative (Obu et al., 2021).

The peatland at Abisko-Stordalen (68.35, 19.05), hereby referred to as Stordalen, is a palsa bog that predominantly relies on precipitation, resulting in ombrotrophic conditions. The site falls within the discontinuous permafrost zone and features elevated palsas underlain by permafrost and permafrost-free waterlogged depressions. Recent climate warming has accelerated permafrost degradation and led to the collapse palsas (Johansson et al., 2011). The plant community composition is controlled by soil water content and topography, where palsas are dominated by dwarf shrubs like crowberry *Empetrum hermaphroditum*, lingonberry *Vaccinium vitis-idaea*, and cloudberry *Rubus chamaemorus*, and wet and semi-wet depressions are covered by Carex sedge and Eriophorum cottongrass (ICOS n.d.). Peat initiation started between 4700-6000 calendar years before present (cal. BP) in the southern and northern part respectively, and the peat depth ranges from 1 to 3 metres with permafrost typically found at depths beyond 0.5-1 m (Chaudhary et al., 2017b; ICOS, n.d.). The mean annual temperature (MAT) is -0.1°C and the mean annual precipitation (MAP) is 332 mm (1981-2010), with a noticeable trend of increasing temperatures and precipitation over the last decades (ICOS, n.d.)

Attawapiskat is situated in the southern part of the Hudson Bay Lowlands (52.7, -83.95), where peat started forming around 8000 cal BP (Packalen et al., 2016). The area is distinguished by fen and bog peatlands with peat depths ranging from 1 to 4 metres storing approximately 100 kg of carbon per square metre (Helbig et al., 2019). The study site is a low-shrub bog characterised by raised hummocks mainly covered by Sphagnum mosses and lichens, and wet, lower-lying areas where lichens are less abundant and with various Sphagnum species and sedges dominate the landscape (Helbig et al., 2019). The site lies within a discontinuous permafrost region with a MAT of -1.3 °C and a MAP of 700 mm (Todd & Humphreys, 2022).

The Scotty Creek bog (61.308, -121.298) is located in continental western Canada, an area where permafrost occupies about 45% of the landscape which results in a varied terrain of raised forested permafrost plateaus, permafrost-free wetlands, and lakes (Sonnentag et al., 2020; Quinton et al., 2011). The site is a collapse-scar bog, created by thawing permafrost that causes the ground to subside into waterlogged depressions. The bog is mainly covered by Sphagnum mosses and bryophytes with occasional ericaceous shrubs, pod grass, and spruce (Helbig et al., 2017). Peat accumulation in the area began around 8500 cal BP and the current peat depth varies between 2-8 metres (Haynes et al., 2019; Talbot et al., 2017). Scotty Creek is characterised by a dry, subarctic climate with a MAT of -2.8 °C and MAP of 388 mm (Sonnentag & Quinton, 2021). Climate data have shown temperatures increasing nearly four times faster than the global average and high rates of permafrost thaw leading to a rapid expansion of wetlands over the recent decades, while precipitation has not increased significantly (Chartrand et al., 2023; Quinton et al., 2019).

The Mer Bleue bog (45.407, -75.484) is situated in a cool-temperate region that resembles boreal raised shrub bogs, and peat accumulation was initiated about 8400 cal BP. It started as a fen and transitioned into a bog approximately 6800 to 7100 calendar cal BP (Roulet et al., 2007). Peat depths range from 5-6 metres, shaping the landscape with hummocks and hollows, covered mainly by Sphagnum mosses and a blend of evergreen and deciduous shrubs (Frolking et al., 2010; Roulet et al., 2007). The climate is characterised as cool continental, with a MAT of 6.0 °C and MAP of 943 mm (1971-2000).

Table 1. Information about the study sites, including peatland type, permafrost occurrence, climate, peat initiation and peat depth.

Site name	Site type	Climate	Permafrost	Peat initiation	Peat depth
Stordalen, Sweden	Palsa bog	Subarctic/ tundra	Sporadic	4700 cal B. P	1-3 m
Attawapiskat, Canada	Low-shrub bog	Subarctic	Sporadic	8000 cal B. P	1-4 m
Scotty Creek, Canada	Collapse-scar bog	Subarctic	Sporadic	8500 cal B. P	2-8 m
Mer Bleue, Canada	Ombrotrophic bog	Temperate	No	8400 cal B. P	4-6 m

3.2 Model settings

The model was run in cohort mode, a vegetation mode where each average individual represents an age class (cohort) of a PFT in a patch. In the cohort mode, multiple replicate patches are simulated to ensure a heterogeneity resulting from variations in plant growth, mortality, and disturbance. The current setup included five replicate patches covering an area of 1000 m^2 each. The model is initiated with a patch of varying height to allow for hydrological distribution of water between them. The model allows water to flow laterally between the patches based on a scheme where water flows from elevated patches, hummocks, to low depressions, hollows, which in turn affects the productivity and decomposition of each patch. The different patches also interact and compete for essential resources such as light and space, with some gaining height over time as a result of the interactions between patches while others remain unaffected or decrease in height. The dynamic height adjustment of the patches affects how water is transported from elevated sites to lower depressions through lateral flow, and the changing WTP influences the vegetation occurrence and its biogeochemical characteristics. The average return time of generic patch-destroying disturbances was set to 100 years. The model considers specific plant functional types (PFTs) to represent the common vegetation structures in peatlands. The PFTs that were included in the simulations, namely mosses, graminoids, low summer-green shrubs, low evergreen shrubs, and high summer-green shrubs, encompass different groups of plant species with similar functional and morphological characteristics. The model was initialised for 500 years from bare ground conditions to build up vegetation, soil carbon, and nitrogen pools by recycling the first 30 years of Holocene climate data (see section 3.3.1).

3.3 Simulation descriptions and data requirements

Hindcast and future climate scenarios were simulated in the peatland version of LPJ-GUESS and included three distinct forcing scenarios. The hindcast simulations were forced with Holocene data from the time of peat initiation until 1900, followed by historical data from until 2005. From 2006, future climate was simulated by incorporating bias corrected CMIP5 climate projections until the year 2100. Every simulation that was performed ran from peat initiation until 2100.

3.3.1 Hindcast simulations

The hindcast simulations ran from peat initiation until 2005 and included two forcing periods: Holocene climate data until 1900 and historical climate data until 2005. The establishment of peat was determined using data from Chaudhary et al., 2020, where a surface dataset of peat basal ages was compiled by interpolating 5000 data points obtained from existing datasets. Basal peat refers to the base layer of peat in a peatland from which the age represents the time since the initiation of peat accumulation at that specific location. The basal age nearest the studied peatlands were derived from the dataset and determined the length of the hindcast simulation.

Holocene climate data containing data from 10 kyr before present until 1900 obtained from Chaudhary et al 2020 was used to force the model until 1900 (Fig. 3). Temperature and precipitation data was generated by the delta-change method, where climate anomalies from

the Hadley Centre's Unified Model were applied to monthly historical CRU TS 3.0 global gridded climate dataset between 1900 and 1930 to create monthly climate forcing series (Miller et al., 2008). Historical mean annual temperature (MAT) and mean annual precipitation (MAP) from the CRU dataset for each peatland are presented in Fig. 3a and Fig. 3b. CRU data of cloudiness between 1900 and 1930 were repeated throughout the dataset and all data was later interpolated to daily values. A detailed description is available in Chaudhary et al., 2020.

The model was forced with the CRU TS 3.0 monthly global gridded climate dataset from 1901 to 2005 (Fig. 4) (Mitchell & Jones, 2005). The dataset has a global coverage and a spatial resolution of 0.5°. The CRU data was evaluated against observed measured climate datasets for each site to check for biases. Daily observed climate data from the closest weather station to each site (Table 2) was retrieved from the Swedish Meteorological and Hydrological Institute [SMHI] and the Canadian Centre for Climate Services [CCCS]. First, monthly mean temperature and monthly total precipitation were computed for the available timespan. Second, the monthly observations were compared to CRU and RMSE was computed. A linear regression analysis was additionally performed to evaluate the relationship between the observed and modelled climate using R^2 statistics.

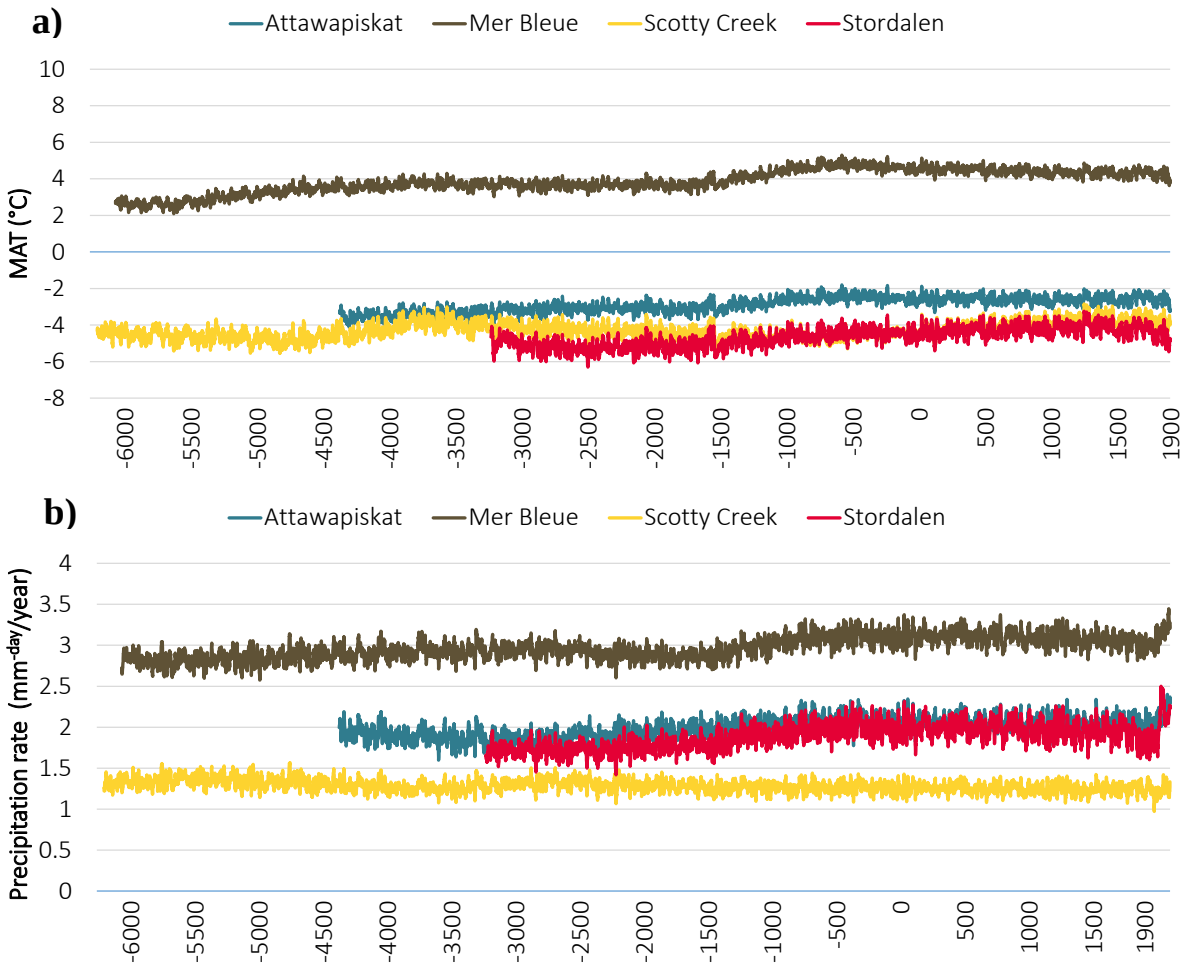

Figure 3. Holocene a) mean annual temperature (MAT) and b) mean annual precipitation rates from local peat initiation until 1900 at each peatland. Precipitation rates are given in mean daily

precipitation rate per year and temperature in °C. A moving average of 10 years has been applied to smooth the data.

Table 2. Climate stations used to retrieve historical climate data for each site to use for evaluation of the historical CRU dataset. The temporal scope refers to the time period used to evaluate the CRU data.

Site name	Source	Climate station name	Distance from site	Temporal scope
Stordalen	SMHI, n.d.	Abisko	10 km	1913–2003
Attawapiskat	CCCS, n.d.	Attawapiskat	105 km	1968 (Oct-Dec)
Scotty Creek	CCCS, n.d.	Fort Simpson	60 km	1901-1963
Mer Bleue	CCCS, n.d.	Ottawa CDA	20 km	1901-2000

Holocene CO_2 concentrations until 1850 were obtained from Chaudhary et al. 2020, where they were computed using boundary conditions in the UM time slice experiments (Chaudhary et al., 2020; Miller et al., 2008). From 1850 to 2000, observed annual CO_2 concentrations from atmospheric or ice core measurements were used. The data was obtained from the European Environment Agency and was available at five-year time steps and were interpolated linearly to obtain annual values (EEA, 2019).

3.3.2 Climate change simulations

Each climate change simulation was forced with data from 2006 until 2100 (Fig. 4). The future climate projections for each RCP scenario were obtained from CMIP5 runs with the IPSL-CM5A-LR model and included the low-emission scenario RCP2.6 and high emission scenario RCP8.5. The model has an equilibrium climate sensitivity (ECS) of 4.1°C, which is 0.9 °C higher than the CMIP5 model mean and implies that the model predicts a greater warming potential compares to the mean for a given increase in GHG concentrations (Flato et al., 2013). Daily mean temperature and total precipitation from 2006-2100 were retrieved from the ISIMIP repository which offers daily climate data bias-adjusted to observation data from the EWEMBI dataset (Lange & Büchner, 2017). Time series of climate data was retrieved from the grid closest to each site, and the units were converted from Kelvin to °C for temperature and from kg m^{-2} s^{-1} to mm^{-day} for precipitation. Future mean annual temperature (MAT) and mean annual precipitation (MAP) for each RCP scenarios are presented in Fig. 4a and Fig. 4b. Future CO_2 concentrations for each RCP scenario under CMIP5 were obtained from the International Institute for Applied Systems Analysis's RCP database (IIASA, 2009). Each scenario included data from 2000 to 2100 in time steps of five or ten years. The data for each RCP scenario were interpolated linearly between each time step to retrieve annual values up to 2100.

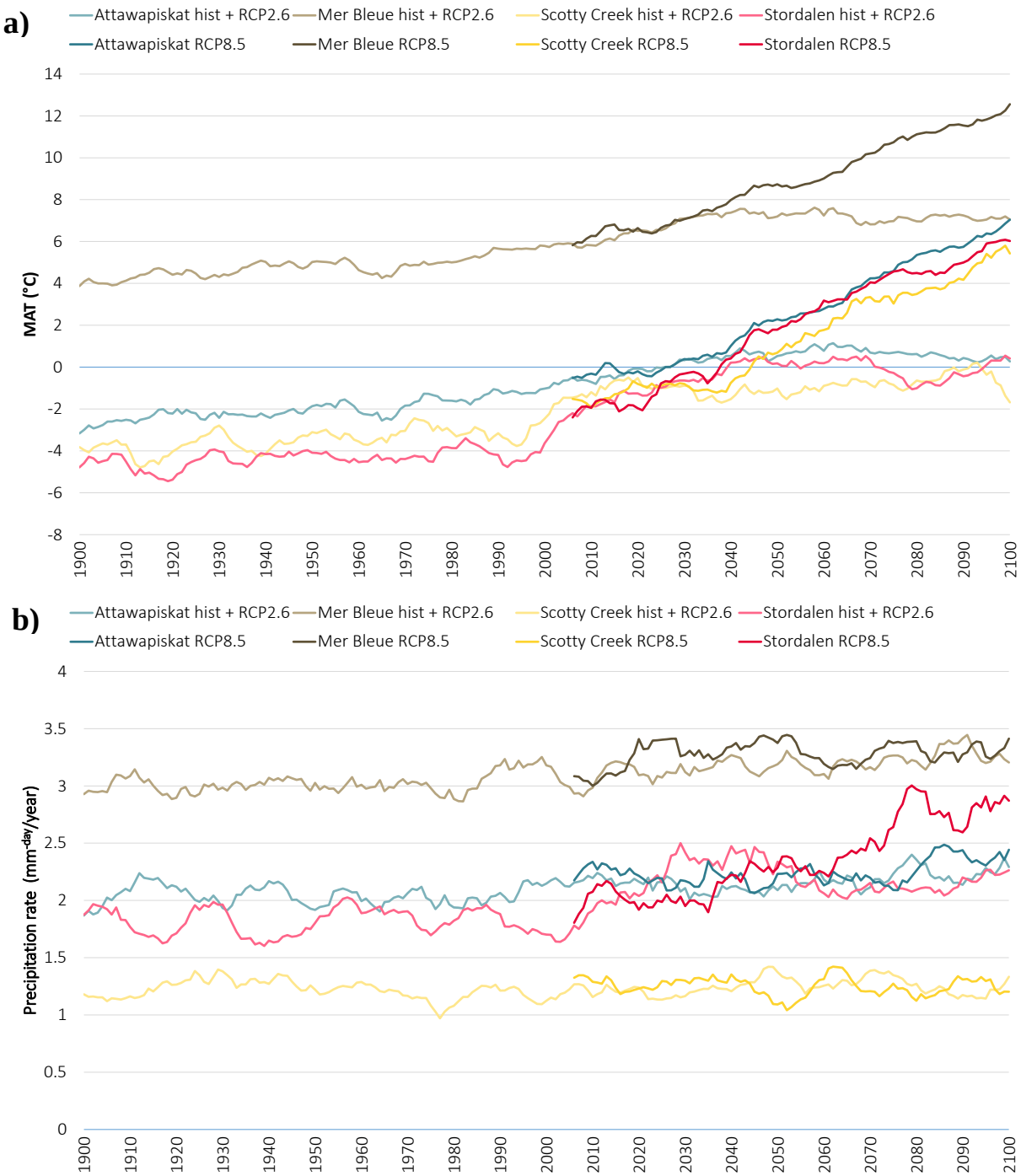

Figure 4. Historical and future a) mean annual temperature (MAT) and b) mean annual precipitation rates from 1900 until 2100 at each peatland. Precipitation rates are given in mean daily precipitation rate per year and temperature in °C. Climate data between 1900 and 2005 is based on gridded observations from CRU TS 3.0, and data from 2006 onwards is based on CMIP5 projections. The two RCP scenarios RCP2.6 (light colours) and RCP8.5 (dark colours) are visualised from 2006 onwards. A moving average of 10 years has been applied to smooth the data.

3.3.3 Analysis of the climatic controls

An analysis of the climatic controls was performed to quantify the importance of the climatic drivers that are responsible for modulating carbon fluxes. This was achieved by running multiple model simulations using single climate forcings, i.e., only temperature, only

precipitation, and only CO_2, to identify which of the three variables influence the carbon dynamics the most and to identify possible differences between the sites. Each simulation was initially driven by combined historical climate data from the onset of peat initiation until 2005. Subsequently, starting from 2005, the model was subjected to individual climate forcings projections under RCP8.5 one at a time, while the other remained constant according to a non-forcing scenario. Non-forcing files were created to be able to isolate the effects of using a single climate forcing in a simulation. The non-forcing CO_2 data was created by repeating the CO_2 concentration in 2006, and detrended future temperature and precipitation were used as non-forcing climate data. Detrending temperature and precipitation was performed in R, the former using the *detrend* function of the ASTSA package where a linear trend is fitted and subtracted from the dataset (Stoffer & Poison, 2023). Detrending of precipitation data is incompatible with subtraction methods since it often results in negative values. The detrending of precipitation was thereby performed using the multiplication method outlined in O'Brien & Nolan (2023). Linear regression analysis between the responses of net ecosystem productivity (NEP), CH_4, GPP, and R_{eco} to all forcings and single forcings were conducted and R^2 and RMSE were computed.

3.4 Evaluation of results

Model output, including carbon accumulation rates (CAR), NEP, CH_4 emissions and active layer depth (ALD) were evaluated against observations. These observations were derived from measurements and data analysis techniques such as eddy-covariance, chambers, and peat cores. The evaluated NEP incorporates the influence of fire occurrence and vegetation establishment, as well as the influence of GPP and R_{eco}. The LPJ-GUESS peatland model has been rigorously tested and validated against observed data, including peat depth, vegetation composition, ALD, ecosystem carbon fluxes, and carbon accumulation rates, across regions in Scandinavia and Mer Bleue, demonstrating favourable performance (Chaudhary et al., 2017a, 2017b).

4. Results

4.1 Evaluation of historical model results

Comparison with observational data in literature shows that modelled NEP that includes fire disturbance and vegetation establishment is overestimated, yielding more positive values and thereby lower sink capacities compared to site-specific and regional observations. In a review by Frolking et al., 2011, observed NEE and CH_4 emissions from global northern peatlands indicate NEE ranging between -20 to -100 g C m^{-2} y^{-1}. This aligns with modelled historical NEP in Stordalen and Attawapiskat (Table 3). However, historical NEP between 1900 and 2000 does not align with observations in Mer Bleue and Scotty Creek, where both are modeled as consistent carbon sources. On the contrary, the calculated net difference between GPP and R_{eco} that disregards fire disturbance and vegetation establishment results in higher carbon sink capacities compared to observations, as it ranges between -130 and -270 g C m^{-2} y^{-1} across the studies sites around 2000 (Table 3). Stordalen is closest to observations with -130 g C m^{-2} $y^{-1.}$ Although all sites are modelled accurately as consistent carbon sinks, the annual carbon sinks are much greater than observations. Similar trends are observed in

comparison to local observations at the study sites. In Mer Bleue, modelled average NEP between 1998 and 2004 was 56 g C m^{-2} y^{-1}, outside the observed range of −40.2 ± 40.5 g C m^{-2} y^{-1} in the same period (Roulet et al., 2007). The model suggests a strong carbon source, while observations indicate a sink. In Attawapiskat, the modeled average NEP is about 22 g C m^{-2} y^{-1}, contrasting with observed values of −52 ± 16 and −80 ± 14 g C m^{-2} y^{-1} at fens and bogs between 2011 and 2015 (Helbig et al., 2019). The modelled NEP in Scotty Creek is also higher than site observations, with -11 and 70 g C m^{-2} y^{-1} under RCP2.6 and RCP8.5 respectively, compared to observations of -23.5 g C m^{-2} y^{-1} (Helbig et al., 2017). Good agreement is found for Stordalen, where the average NEP which aligns with site observations (Table 3). Despite some annual comparisons showing agreement, the NEP across the studied peatlands is generally more positive compared to observations at the Canadian peatlands, suggesting an underestimation in carbon sink capacities present in historical results when forced with CRU data.

Table 3. Comparison of modelled and observed net ecosystem productivity (NEP) based on observations found in literature.

Variable	Reference	Geographical area	Temporal range	Observed values (g C m^{-2} y^{-1})	Modelled values (g C m^{-2} y^{-1})
NEP	Frolking et al., 2011	Global northern peatlands	Based on papers published between 1999-2011	-20 to -100	–70 to +80 all sites (NEP) -130 to -270 all sites (NEE)
NEP	Roulet et al., 2007	Mer Bleue	1998-2004	−40.2 ± 40.5	-2.9 to +88.5 (average 56)
NEP	Helbig et al., 2019	Attawapiskat	2011-2015	−52 ± 16 (fens) and −80 ± 14 (bogs)	-25.2 to +53.5 (average 22)
NEP	Helbig et al., 2017	Scotty Creek	2016	-23.5	-11
NEP	Yu, 2012	Stordalen	2008-2009	-50 ± 17.0	-55 and -59

Modelled CH_4 fluxes agree with regional observations but are higher than site-specific observations. The average modelled CH_4 emissions between 1900 and 2000 aligns well with observed CH_4 fluxes from northern peatlands (Table 4). The modelled CH_4 flux in Attawapiskat agrees with modern observations in the HBL (Table 4). In Stordalen, Holmes et al., 2022, and Łakomiec et al., 2021 observed annual CH_4 fluxes from 2012 to 2018 ranging between 0.3 - 19.2 and 2.2 - 9.7 g C m^{-2} y^{-1}, respectively. In contrast, the modelled flux for the same period ranges between 2.4 - 51.2 g C m^{-2} y^{-1}. However, the modelled flux is lower than observations from ICOS from 2014, with an observed flux of 8.6 and a modelled flux of 2.5 g C m^{-2} y^{-1} (Rinne & ICOS Sweden, 2021). The modelled CH_4 fluxes in Mer Bleue and Scotty Creek are also higher than observations. In Mer Bleue, the modelled average CH_4 flux was

53.1 g C m^{-2} y^{-1} between 1998 and 2004, compared to observations of 3.7 ± 0.5 g C m^{-2} y^{-1} (Roulet et al., 2007). Measurements between 2013 and 2017 in Scotty Creek resulted in an average flux of 8 ± 1 g C m^{-2} y^{-1}, significantly lower than the modelled flux of 45 g C m^{-2} y^{-1} (Sonnentag et al., 2020). Although the lower values are consistent with observations, the model simulates higher maximum CH_4 fluxes and exhibits a higher annual variation. This increased variation poses challenges when evaluating results for a single year alongside observational data.

Table 4. Comparison of modelled and observed methane emissions (CH_4) based on observations found in literature and datasets

Variable	Reference	Geographical area	Temporal range	Observed values (g C m^{-2} y^{-1})	Modelled values (g C m^{-2} y^{-1})
CH_4	Frolking et al., 2011	Global northern peatlands	Based on papers published between 1980-2010	1 to 52	1 to 63
CH_4	Packalen et al., 2014	Hudson Bay Lowlands	2009–2011	1 to 50	24 to 56 (average 37) in Attawapiskat
CH_4	Holmes et al., 2022,	Stordalen	2012-2018	0.3 to 19.2	2.4 - 51.1 (average 21.4)
CH_4	Łakomiec et al., 2021	Stordalen	2014-2016	2.2 - 9.7	2.5 - 51.2 (average 26.9)
CH_4	Rinne & ICOS Sweden, 2021	Stordalen	2014	8.6	2.5
CH_4	Roulet et al., 2007	Mer Bleue	1998-2004	3.7 ± 0.5	51.1 to 54.9 (average 53.1)
CH_4	Sonnentag et al., 2020	Scotty Creek	2013-2017	8 ± 1	38.7 to 51.1 (average 45.2)

LARCA and ALD in the model are generally in line with observations for most sites. The modelled ALD in Stordalen and Attawapiskat aligns with historical observations but is much larger than observations in Scotty Creek, consistent with issues encountered in previous modeling studies (Brown, 1973; Johansson et al., 2006; Qiu et al., 2022). The model tends to slightly underestimate LARCA in Scotty Creek, where the 1900-2000 average is 1.8 and 0.4 g C m^{-2} y^{-1} lower than observations (Talbot et al., 2017; Yu et al., 2009). In Attawapiskat, the modeled average LARCA from 6000 cal BP until 2000 aligns with nearby observations (Bunbury et al., 2012). In Mer Bleue, the modelled LARCA between 3000-400 cal B.P is 1.9 g C m^{-2} y^{-1} larger than observations from peat core analysis (Roulet et al, 2007).

The historical species composition was evaluated by comparing modelled LAI per PFT with vegetation compositions found in literature. Observations from Stordalen show that

palsas are primarily inhabited by dwarf shrubs, while wet depressions are characterized by sedges and cottongrass. The model did not simulate graminoids until the late 20th century, contrary to observations which indicate their presence already in the beginning of the century. Mosses and low shrubs were the predominant vegetation in the model, consistent with observations. In Attawapiskat, observations reveal that the peatland consists of hummocks covered by Sphagnum mosses and lichens, and wet depressions covered by Sphagnum species and sedges. The model simulations accurately represent mosses and graminoids as dominant vegetation. In Scotty Creek, observations indicate that the bog is primarily covered by Sphagnum mosses and bryophytes, with occasional occurrences of ericaceous shrubs, pod grass, and spruce. However, the model includes very few mosses, in contrast to observations where they are dominant. Instead, the model suggests graminoids and spruce as dominant species. In Mer Bleue, observations primarily feature Sphagnum mosses and a mixture of evergreen and deciduous shrubs. However, the model predominantly simulated mosses and spruce, with very few shrubs, potentially indicating an underrepresentation of shrubs compared to observations. Additionally, the model includes graminoids, which are not mentioned in the observations.

4.2 Evaluation of historical climate data

The results from evaluating historical CRU climate data against observations reveal differences in CRU temperatures, with RMSE ranging between 3.1 and 4.5 (Table 5). Notably, CRU temperatures were consistently colder than observations. Although the highest R^2 was observed in Attawapiskat, it should be noted that only three months of data were available, making the resulting statistics unrepresentative of the accuracy at the site. Conversely, CRU temperatures in Mer Bleue exhibited the best agreement with observational data, albeit with a relatively high RMSE of 3.1 (Table 5). In the case of precipitation, lower R^2 values and higher RMSE values were observed, indicating a relatively poor fit between the observed and CRU precipitation data.

Table 5. Computed R^2 and RMSE for the difference between observed historical climate and CRU data at each site. The analysis is based on data between 1913- 2003 for Stordalen, 1968 (October – December) for Attawapiskat, 1901-1963 for Scotty Creek, and 1901-2000 for Mer Bleue.

	Temperature (°C)			Precipitation (mm/month)		
	R^2	RMSE	Bias	R^2	RMSE	Bias
Stordalen	0.7946	3.8	Colder	0.0032	31.8	Less precipitation
Scotty Creek	0.9089	3.9	Colder	0.1033	32.0	Less precipitation
Mer Bleue	0.9336	3.1	Colder	0.0029	46.6	Less precipitation
Attawapiskat	0.9998	4.5	Colder	0.5419	32.8	Less precipitation

4.3 Historical carbon stocks and fluxes

The magnitude of the historical carbon pools and carbon accumulation rates (CAR) differed both spatially and temporally. The initial carbon pools at the start of each simulation were large across the Canadian sites and decreased to stabilize approximately after 1000 years (Fig.

5). The largest ecosystem carbon pool between 1900 and 2000 was observed in Scotty Creek, followed by Attawapiskat, while Stordalen exhibited the smallest carbon pool (Table 6). Although large in magnitude, the carbon pool in Scotty Creek decreased from 26.0 kg C m^{-2} between 1900 and 1950 to 24.6 kg C m^{-2} between 1950 and 2000, which is reflected on the negative average CAR (Table 6). Negative CAR was also observed in Mer Bleue, where the carbon pool decreased from 10.4 to 8.9 kg C m^{-2} in the second half of the century (Table 6). Contrary to the previous sites, the carbon pools in Stordalen and Attawapiskat remained stable throughout the century, as they accumulated carbon at an average rate of 58.5 and 18.9 g C m^{-2} y^{-1}, respectively (Table 6). Despite the high CAR in Stordalen, the ecosystem carbon pool remained very small around below 1 kg C m^{-2} throughout the century.

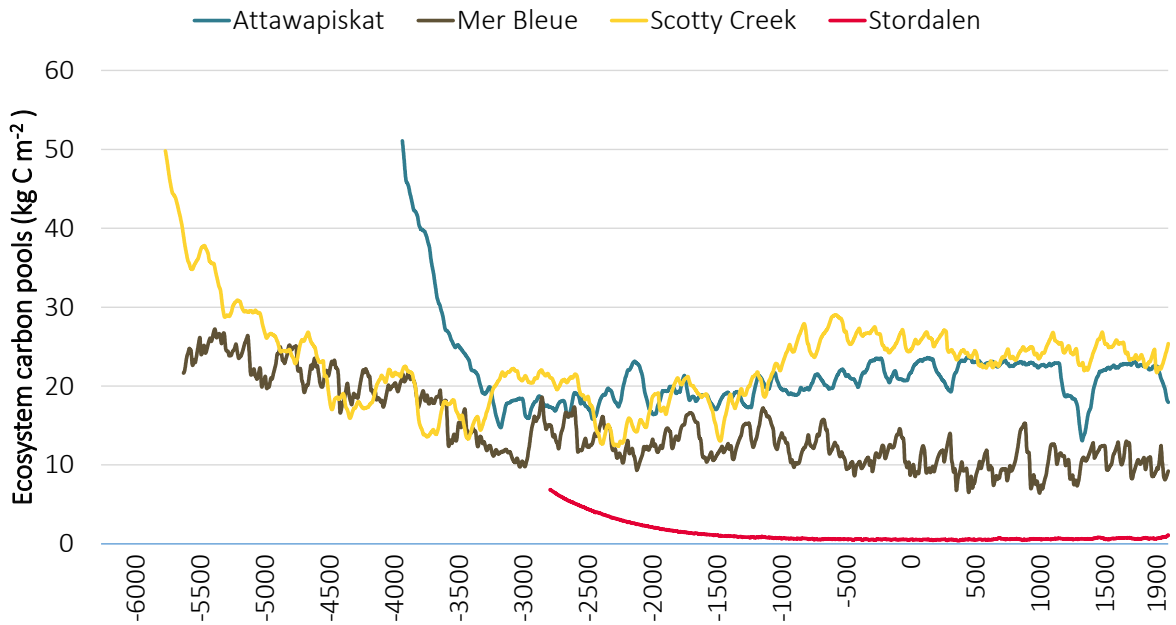

Figure 5. Total ecosystem carbon stocks from peat initiation until 1900 with units in kg C m^{-2}. The ecosystem carbon stock includes carbon from litter, soil organic matter, and vegetation. The graph excludes the first 500 years after peat initiation since all plant functional types (PFTs) accumulate a lot of carbon in the spin up period, which then stabilizes in the first 500-1000 years. The decrease in carbon stocks in the initial stages of each peatland are attributed to this stabilization.

Table 6. Modelled carbon accumulation (CAR) between 1900-2000 with units in g C m^{-2} y^{-1} and modelled ecosystem carbon pools in kg C m^{-2} averaged over 1900-1950 and 1950-2000. The ecosystem carbon pool includes carbon from litter, soil organic matter, and vegetation.

Site	CAR (1900-2000)	Carbon pool (1900-1950)	Carbon pool (1950-2000)
Stordalen	58.5	0.72	0.9
Scotty Creek	-9.9	26.0	24.6
Mer Bleue	-45.7	10.4	8.9
Attawapiskat	18.9	21.5	21.9

The modelled NEP incorporates the influence of fire occurrence and vegetation establishment. Stordalen acted as the largest carbon sink historically among the four sites, with an average NEP of -58 g C m^{-2} y^{-1} between 1900 and 2000 (Fig. 6). Stordalen's annual soil ice fraction, a proxy for permafrost occurrence, remained stable around 70% across the century, indicating the highest permafrost occurrence among the study sites. A small decrease in soil ice fraction at the end of the century coincided with a deepening of ALD from -0.5 to -0.8 m. The high permafrost occurrence and shallow ALD reflected on the low CH_4 fluxes, which remained stable with an average of 4 g C m^{-2} y^{-1} between 1900 and 2000 after which they increased rapidly in line with the change in ALD and ice fraction and increasing temperature (Fig. 7). The vegetation composition remained unchanged with mosses dominating and a small occurrence of low shrubs. Attawapiskat acted as the second largest carbon sink between 1900 and 2000 (Fig. 6). The second-highest soil ice fraction remained stable around 60% during the first half of the century while showing a decreasing trend and higher variation from 1980 onwards. The ALD remained stable throughout the century at around -0.7 m, slightly deeper than observed ALD in Stordalen. The CH_4 fluxes increased throughout the century as graminoids dominated the vegetation composition which also included mosses (Fig. 7). Scotty Creek shifted from acting as an average carbon sink between 1900-1950 to a carbon source between 1950 and 2000, on average acting as a source with positive NEP (Fig. 6). The modelled annual soil ice fraction remained stable at 50% in the first half of the century but decreased across the second half, while ALD remained constant at -1.7 m, the second highest among the sites. The second greatest CH_4 emissions were also observed at the site (Fig. 7). Graminoids and boreal needle leaved evergreen trees were the dominating species at the site. The highest carbon source capacity was observed in Mer Bleue, which acted as a consistent carbon source throughout the century (Fig. 6). No permafrost occurrence was simulated in Mer Bleue (i.e., zero annual soil ice fraction) along with the greatest ALD of -3.3 m and CH_4 emissions (Fig. 7). The vegetation composition was dominated by boreal evergreen trees, followed by graminoids, mosses and low shrubs.

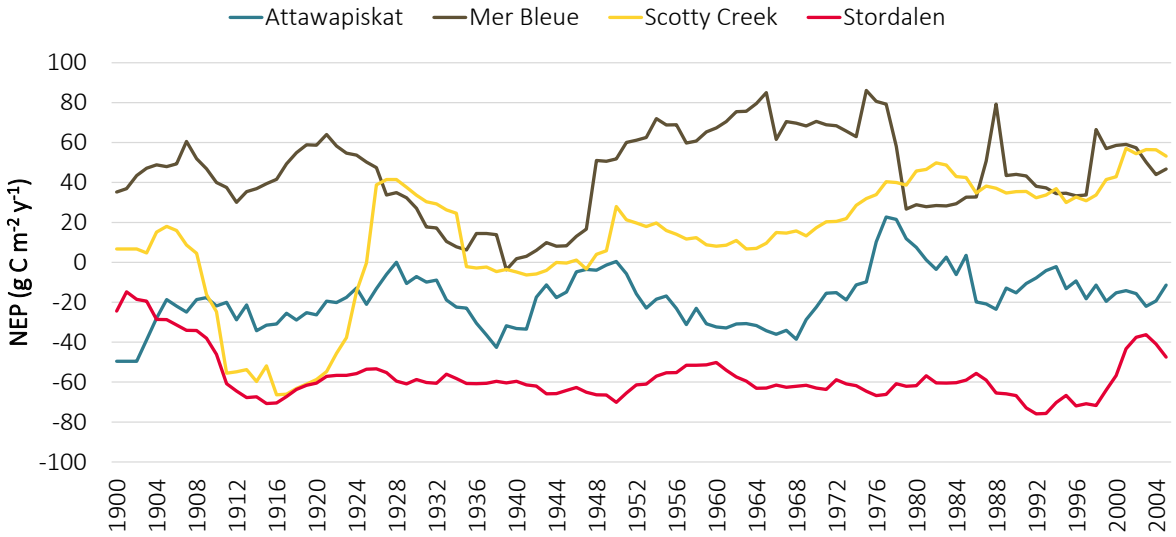

Figure 6. Modelled annual net ecosystem productivity (NEP) between 1900 and 2005 for each site. The modelled NEP incorporates the influence of fire occurrence and vegetation establishment. A moving average of 10 years was applied to smooth the data.

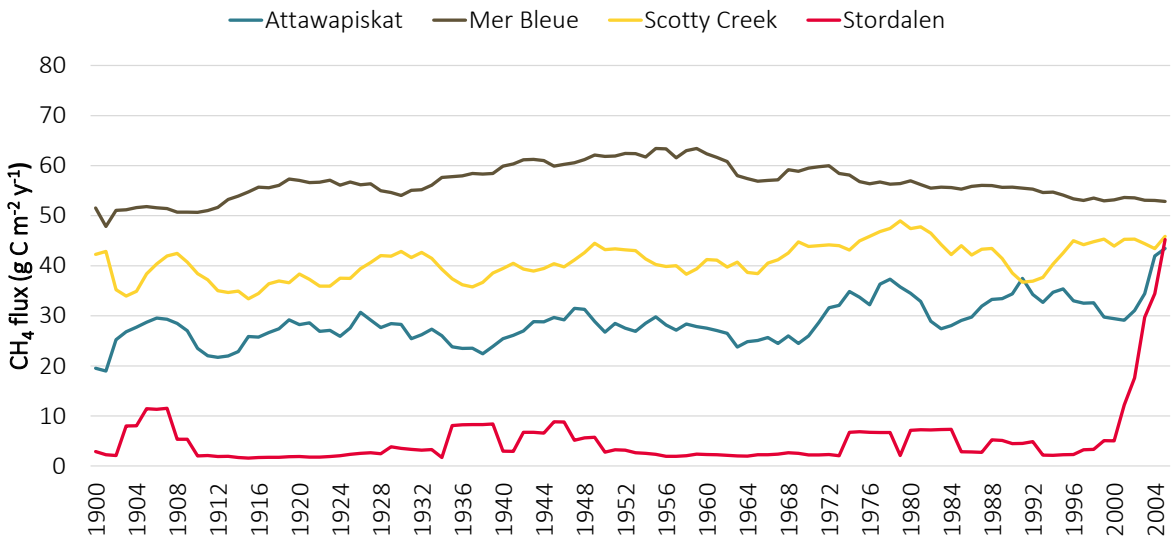

Figure 7. Modelled methane (CH_4) flux between 1900 and 2005 for each site. A moving average of 5 years was applied to smooth the data.

4.4 Future carbon stocks and fluxes

4.4.1 Carbon stocks

The rates of change of future ecosystem carbon pools varied between the sites, with Stordalen being the only site where the carbon pool consistently increased throughout the century under both RCP scenarios. In Stordalen, the carbon stocks increased slightly across both scenarios with a higher increase observed under RCP8.5 (Fig. 8). The magnitude of change remained minor under both scenarios, resulting in average carbon pools of 2.6 and 3.0 kg C m^{-2} under RCP2.6 and RCP8.5, respectively (Table 7). In Scotty Creek, the carbon pool remained stable under RCP2.6 while it decreased after 2060 under RCP8.5 to an average of 22.1 kg C m^{-2} between 2050-2100 (Table 7). The most notable decrease in the carbon pool was observed in Attawapiskat, where carbon pools rapidly decreased from 22 kg C m^{-2} by 2006 to 6-7 kg C m^{-2} by 2100 across both scenarios (Fig. 8). The rapid decrease resulted in a similar sized carbon pool as Mer Bleue by 2100 under RCP2.6, even though the decrease in Mer Bleue was smaller in magnitude. In Mer Bleue, the total carbon pool increased steadily between 2000-2050 across both scenarios, after which it decreased to an average of 9.3 and 6.3 between 2050-2100 under RCP2.6 and RCP8.5, respectively (Table 7).

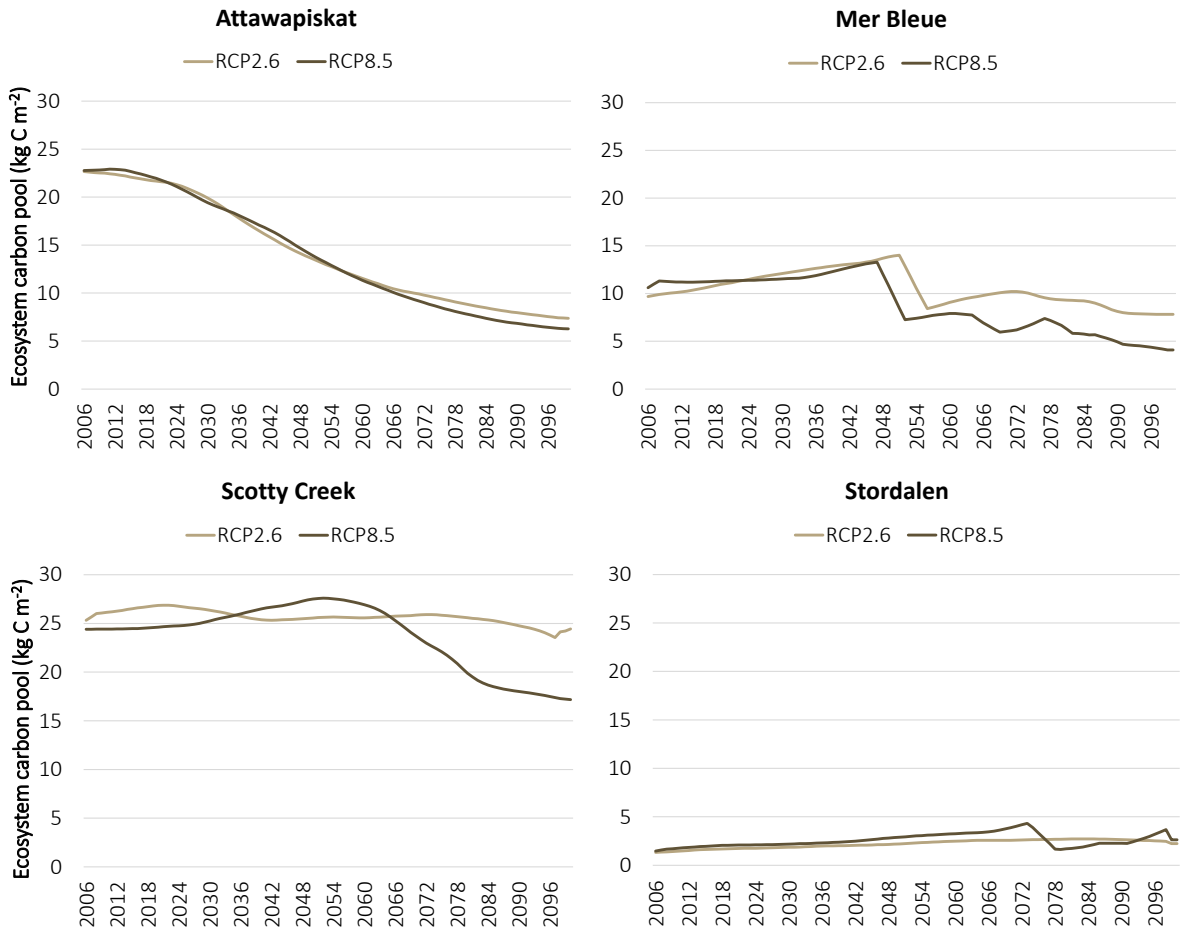

Figure 8. Total ecosystem carbon stocks between 2006 and 2100 with units in kg C m^{-2}. RCP2.6 is visualised in light brown and RCP8.5 in dark brown. The ecosystem carbon stock includes carbon from litter, soil organic matter, and vegetation. Each simulation ran from peat initiation until 2100, resulting in slightly different values by 2006 due to the variation within the model.

Table 7. Modelled annual ecosystem carbon pools (kg C m^{-2}) averaged over the periods 2000-2050 and 2050-2100 under RCP2.6 and RCP8.5. The ecosystem carbon pool includes carbon from litter, soil organic matter, and vegetation.

	RCP2.6 (2000-2050)	RCP8.5 (2000-2050)	RCP2.6 (2050-2100)	RCP8.5 (2050-2100)
Stordalen	1.8	2.2	2.6	3.0
Scotty Creek	26.1	25.4	25.3	22.1
Mer Bleue	11.8	11.7	9.3	6.3
Attawapiskat	19.4	19.6	9.7	9.0

4.4.2 Net ecosystem productivity and its components

To understand the changes in carbon pools, an analysis of the modelled carbon fluxes is crucial. Under RCP2.6, the NEP fluctuated but remained stable under across all sites except Mer Blue (Fig. 9). On the contrary, the sites responded differently to the high forcing scenario

RCP8.5, where the carbon source capacity increased in Stordalen and Mer Bleue, while Attawapiskat increased its carbon sink and Scotty Creek remained stable (Fig. 9). The modelled NEP incorporates the influence of fire occurrence and vegetation establishment.

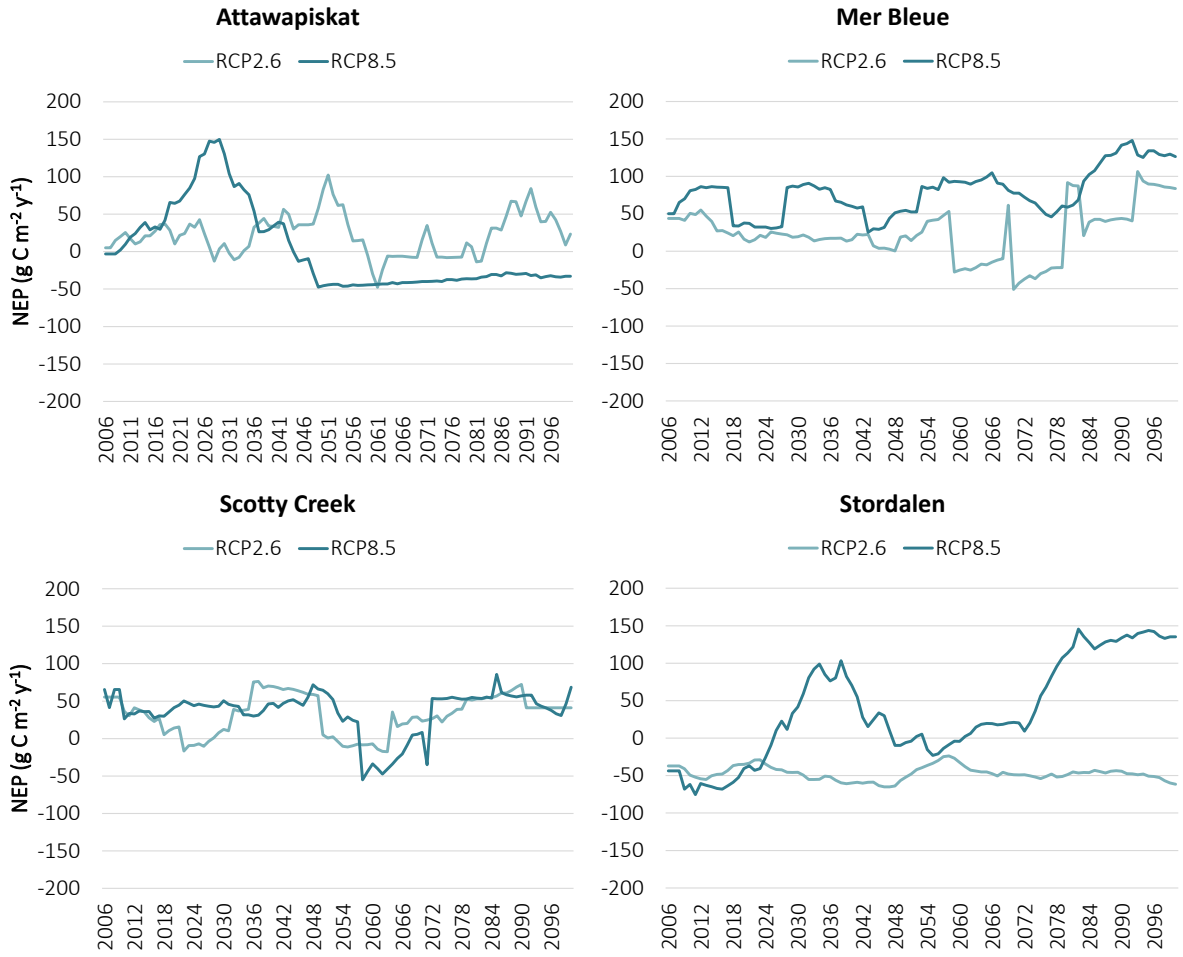

Figure 9. Modelled annual net ecosystem productivity (NEP) between 2006-2100 under RCP2.6 (light blue) and RCP8.5 (dark blue). Positive values indicate a flux towards the atmosphere, i.e., a release of carbon, and negative values indicate a flux from the atmosphere, i.e., an uptake of carbon. The modelled NEP incorporates the influence of fire occurrence and vegetation establishment. Each simulation ran from peat initiation until 2100, resulting in slightly different values by 2006 due to the variation within the model.

Attawapiskat shifted into a carbon source early under both scenarios (Fig. 9). Under RCP2.6, NEP fluctuated but remained at an average of 22 g C m^{-2} y^{-1} between 2000-2100. Interestingly, NEP increases rapidly under RCP8.5 until 2025, from where it decreased to shift into a stable carbon sink about -50 g C m^{-2} y^{-1} by 2045 (Fig. 9). Attawapiskat shifted to become a carbon sink of similar magnitude as historically (between 1900 and 2000) under the high emission scenario. Stordalen remained a carbon sink under RCP2.6 with a NEP around -50 g C m^{-2} y^{-1}, while the site shifted into a carbon source around 2030 under RCP8.5 (Fig. 9). Among all sites, the subarctic site in Stordalen had the potential to become the largest carbon source along with the temperate site Mer Bleue under RCP8.5, with a NEP up to 145 g C m^{-2} y^{-1} by 2100 (Fig. 9). The colder climate at Stordalen resulted in generally lower GPP and R_{eco}

compared to the Canadian sites (Fig. 10). Mer Bleue, which acted as a consistent carbon source already by 1900, increased its carbon source capacity under RCP8.5 (Fig. 9). On the contrary, the NEP decreased under RCP2.6 to shift into a carbon sink but increased again from 2080. Contrary to the aforementioned sites, no notable difference in the response of NEP to the two forcings scenarios was observed in Scotty Creek which indicates a robustness to the degree of climate forcing. Even though the site occasionally functioned as a carbon sink, Scotty Creek remained an average carbon source (Fig. 9). Between 2080-2100, an average NEP of 56 and 61 g C m^{-2} y^{-1} was observed under RCP2.6 and RCP8.5, respectively.

Without considering the impact of vegetation establishment and fire on NEP and instead only analysing the net difference between GPP and R_{eco}, all sites were simulated as robust carbon sinks between 2006-2100 (Fig 10). The results suggest sink capacities ranging between -130 and -275 g C m^{-2} y^{-1} around 2006, with even greater sink capacities observed in some peatlands over the century (Fig. 10). The carbon sink capacity decreased under RCP2.6, mainly driven by decreasing GPP, except for in Mer Bleue where NEP remained stable (Fig. 10). Conversely, an increase in carbon sink capacity was observed in Mer Bleue and Stordalen under RCP8.5 as increasing GPP increased at a faster rate than R_{eco}. Interestingly, the sink capacity in Scotty Creek decreased under RCP8.5 as GPP was observed to decrease in response to the future climate while R_{eco} continued to increase, but still remained a strong carbon sink by 2100 (Fig. 10). The net difference between GPP and R_{eco} in Attawapiskat followed a similar pattern as observed in Figure 8, with a decrease in carbon sink capacity until 2025 driven by decreasing GPP, followed by a stable increase as GPP starts to exceed R_{eco} (Fig. 10). NEP eventually stabilized around -225 and -250 g C m^{-2} y^{-1} (Fig. 10). As GPP surpassed Ecosystem Respiration (R_{eco}) at all peatlands throughout the simulation period, it becomes evident that the influence of fire occurrence and vegetation establishment play significant roles in shaping the overall NEP by influencing vegetation mortality and establishment. In Attawapiskat, fire emissions were generally low throughout the simulation period, while one large fire was simulated in Scotty Creek by 1899, followed by a minor fire in 2087 (Fig. 11). Conversely, Mer Bleue and Stordalen experienced multiple large fires between 2000 and 2100 under the high emission scenario RCP8.5 (Fig. 11).

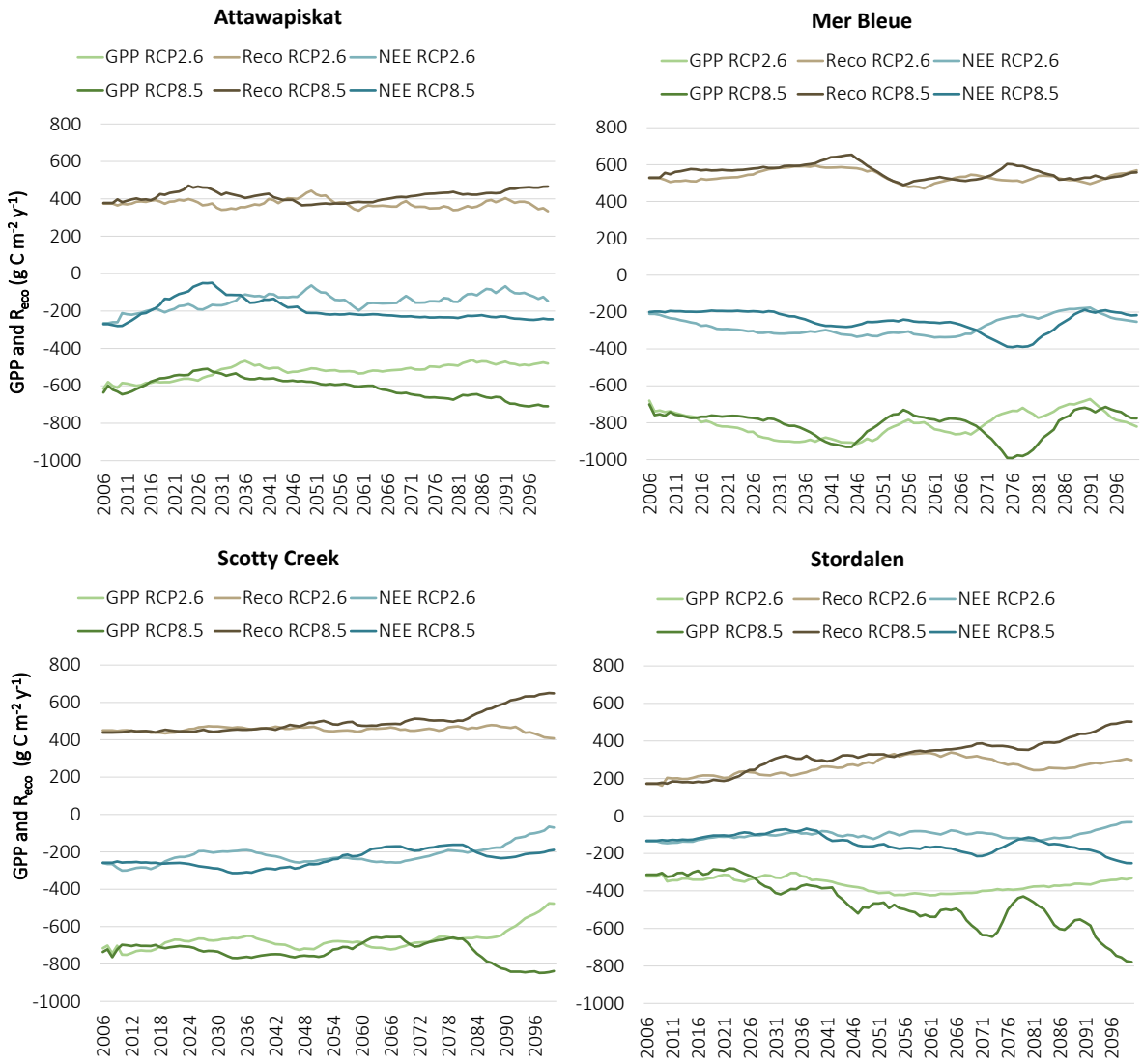

Figure 10. Modelled annual gross primary production (GPP) in green, ecosystem respiration (R_{eco}) in brown, and the computed net ecosystem exchange (NEE) in blue between 2006-2100 under RCP2.6 (light colours) and RCP8.5 (dark colours). The computed NEE is the net difference between the modelled GPP and R_{eco} presented in the graph. Positive values indicate a flux towards the atmosphere, i.e., a release of carbon, and negative values indicate a flux from the atmosphere, i.e., an uptake of carbon.

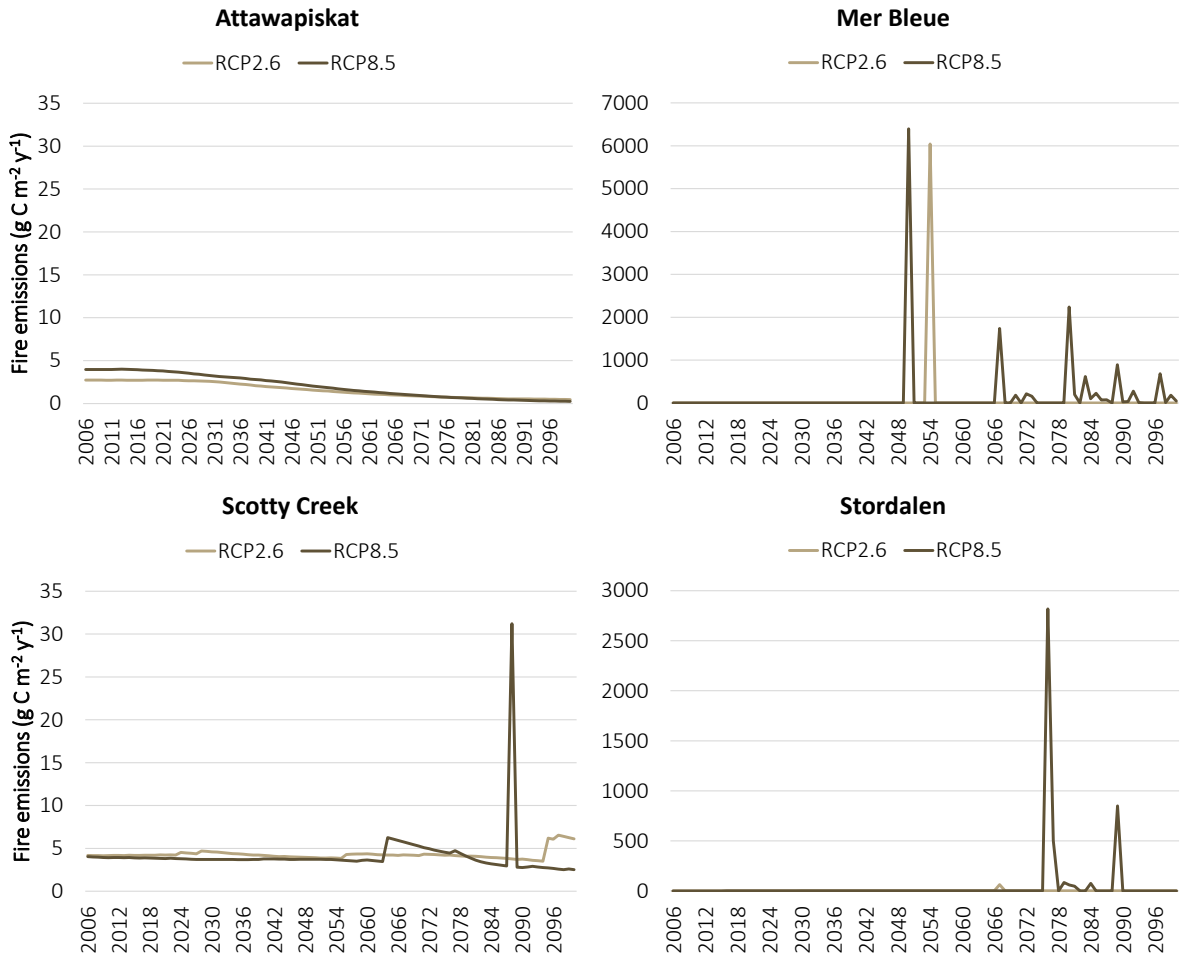

Figure 11. Modelled fire emissions in g C m^{-2} y^{-1} between 2006-2100 under RCP2.6 (light brown) and RCP8.5 (dark brown). The range of values presented on the y axis differ between the sites. Each simulation ran from peat initiation until 2100, resulting in slightly different values by 2006 due to the variation within the model.

4.4.3 Methane emissions, species composition, and permafrost interactions

The annual soil ice fraction exhibited a consistent decrease across all sites under both forcing scenarios. A decrease in soil ice fraction indicates a decrease of frozen soil, which is compensated by a higher fraction of liquid water. Under RCP8.5, the annual soil ice fraction was nearly or completely depleted in all sites before 2100. The decrease coincides with an increasing ALD, i.e. the depth of the soil column that thaws annually, in the three sub-arctic sites with discontinuous permafrost (Fig. 12a). These variables indicate a persistent permafrost thawing across the subarctic sites in response to the projected warming.

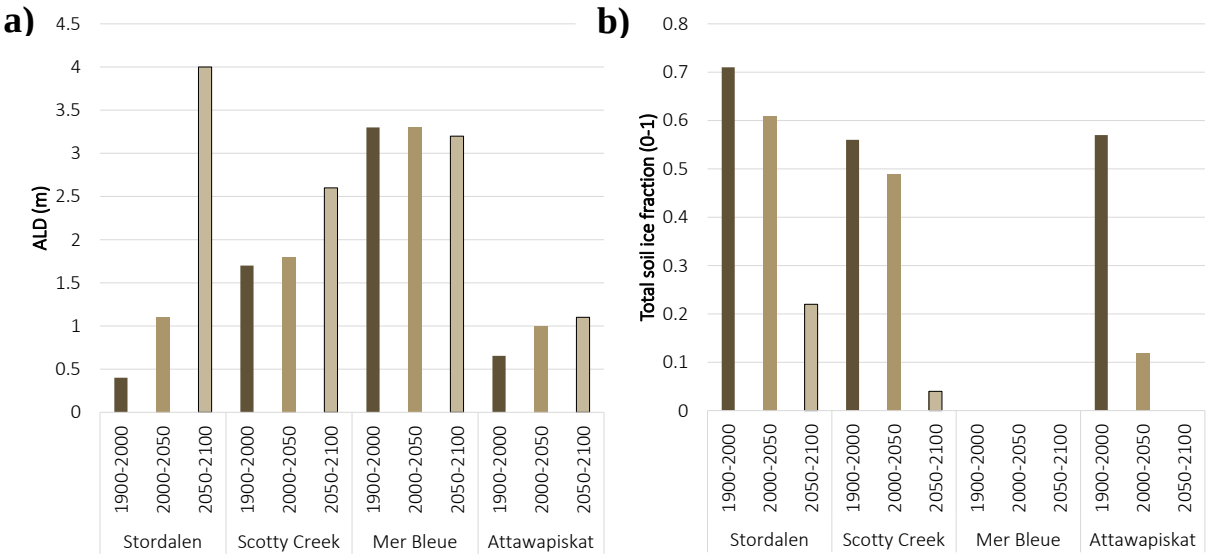

Figure 12. Modelled a) annual active layer depth (ALD) to the left and b) annual soil ice fraction to the right averaged over 1900-2000, 2000-2050 (RCP8.5) and 2050-2100 (RCP8.5).

In Stordalen, the soil ice fraction decreased linearly from 70% by 2000 to 47% and 2% by 2100 under RCP2.6 and RCP8.5, respectively. The decrease corresponded with a similar trend of decreasing ALD, which linearly declined from 0.5 m in 2000 to 4 m by the end of the century under RCP8.5, marking the highest values observed across the sites (Fig. 12a). This suggests a rapid permafrost thaw, typically associated with shallower WTP. Annual WTP remained stable at -25 cm under RCP2.6 and no change in vegetation composition was observed, with mosses dominating the landscape along with minor influence of low shrubs (Fig 13; Fig. 14). Under RCP8.5, shallower WTP were observed after 2050, which was followed by an establishment of graminoids from 2060 onwards (Fig. 13; Fig. 14). Notably, Stordalen exhibited the highest decrease in soil ice fraction and ALD, and the highest increase in CH_4 flux. The CH_4 flux in Stordalen increased from 20 to 60 and 110 g C m^{-2} y^{-1} by 2100 under RCP2.6 and RCP8.5, respectively (Fig. 15).

In Scotty Creek, the soil ice fraction decreased from 46% by 2000 to 20% by 2100 under RCP2.6, while both annual WTP and ALD remained constant, at -130 cm and 1.9 m, respectively (Fig. 12a; Fig. 12b; Fig. 13). The vegetation composition, where coniferous trees and graminoids dominated the landscape, shifted from 2070 as graminoids decreased to be replaced with mosses (Fig. 14). The CH_4 flux remained stable around 50 g C m^{-2} y^{-1} under RCP2.6, coinciding with the constant ALD and soil ice content (Fig. 15). Under RCP8.5, the soil ice fraction decreased rapidly from 2040 to be depleted by 2080 (Fig. 12b). This coincided with a deepening of ALD from 1.8 to 2.8 m and deepening of WTP in the same period (Fig. 13). The change in WTP into less saturated conditions resulted in a rapid shift in vegetation composition where graminoid vegetation disappeared after 2060 and was replaced with mosses and low shrubs (Fig. 14). This in turn affected the CH_4 flux, which decreased from 2045 to stabilize at 39 g C m^{-2} y^{-1} from 2060 onwards, coinciding with the disappearance of graminoids, deepening of WTP, and shift in soil ice and ALD (Fig. 15).

Similarly to Scotty Creek, the CH_4 flux decreased in Attawapiskat throughout the century. The site was modelled to have the smallest CH_4 flux among the sites already by 2020-2040 (Fig. 15). Under RCP8.5, the flux increased up to 50 g C m^{-2} y^{-1} by 2025 before

decreasing to stabilize between 4-9 g C m^{-2} y^{-1} by 2050 (Fig. 15). The decrease in CH_4 emissions coincided with a decrease in soil ice fraction and ALD, where soil ice was depleted by 2045 and ALD stabilized around 1.1 m (Fig. 12a; Fig. 12b). Graminoids dominated the vegetation composition but started to decrease from 2015 to be almost completely replaced by moss by 2050 (Fig. 14). Under RCP2.6, the same transition was observed but started around 2025. Annual WTP was positive under both RCP2.6 and RCP8.5, indicating waterlogged conditions (Fig. 13). The CH_4 flux decreased slightly under RCP2.6, reaching an average of 19 g C m^{-2} y^{-1} between 2080-2100 (Fig. 15). Although soil ice fraction was not completely depleted by 2100, it remained under 3% from 2045, while ALD followed the same trend as observed under RCP8.5 (Fig. 12a; Fig. 12b).

Mer Bleue exhibited increasing CH_4 fluxes under both forcing scenarios, with fluxes projected to increase at a similar pace from 58 to 74 g C m^{-2} y^{-1} under RCP8.5 and from 53 to 68 g C m^{-2} y^{-1} under RCP2.6 (Fig. 15). The CH_4 flux increased as shallower annual WTP was observed under both forcing scenarios, while ALD remained stable throughout the century (Fig. 12a; Fig. 13). The vegetation composition was quite similar under RCP2.6 and RCP8.5, with the landscape being dominated by evergreen coniferous trees, graminoids, and moss. A higher fraction of graminoids and low shrubs were observed to establish under RCP2.6, while more moss established under RCP85 (Fig. 14). Generally, higher LAI was observed under RCP2.6.

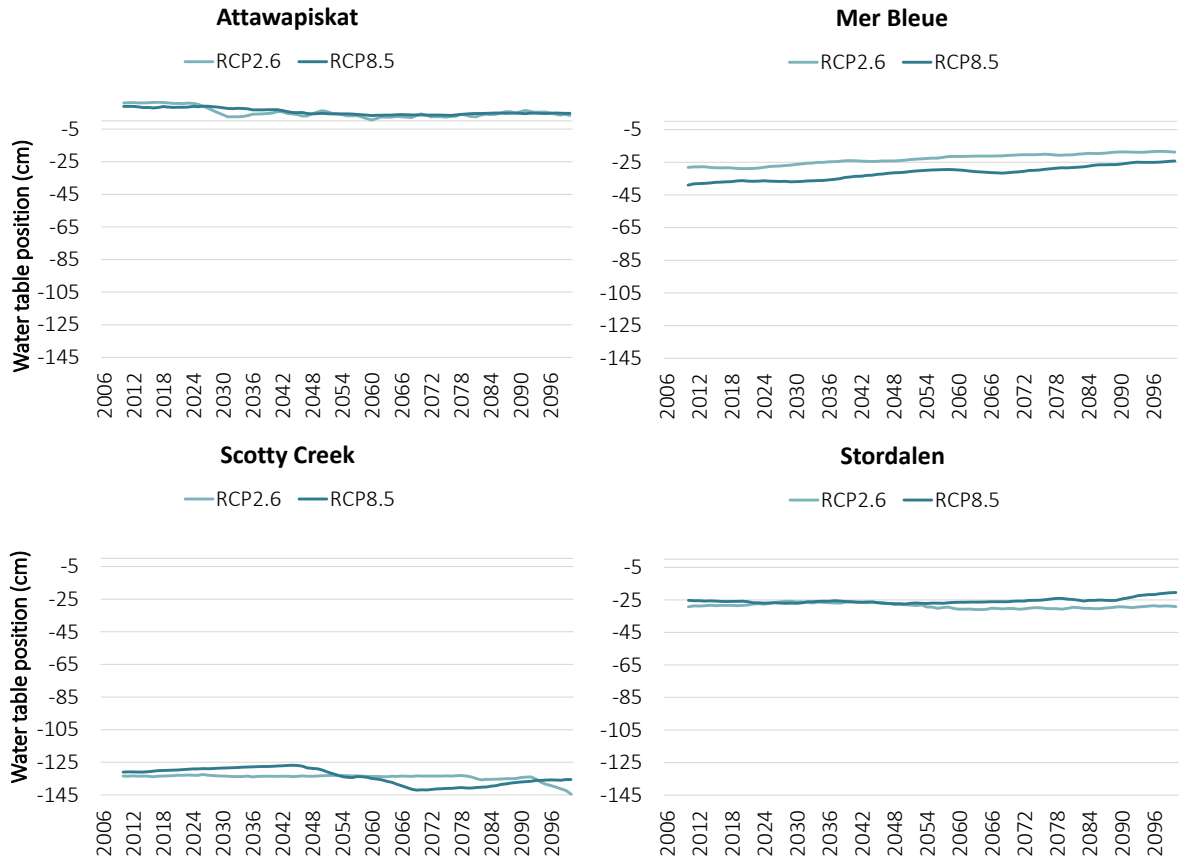

Figure 13. Modelled annual water table position (WTP) between 2006-2100 under RCP2.6 (light blue) and RCP8.5 (dark blue). The negative sign indicates the depth below the soil surface.

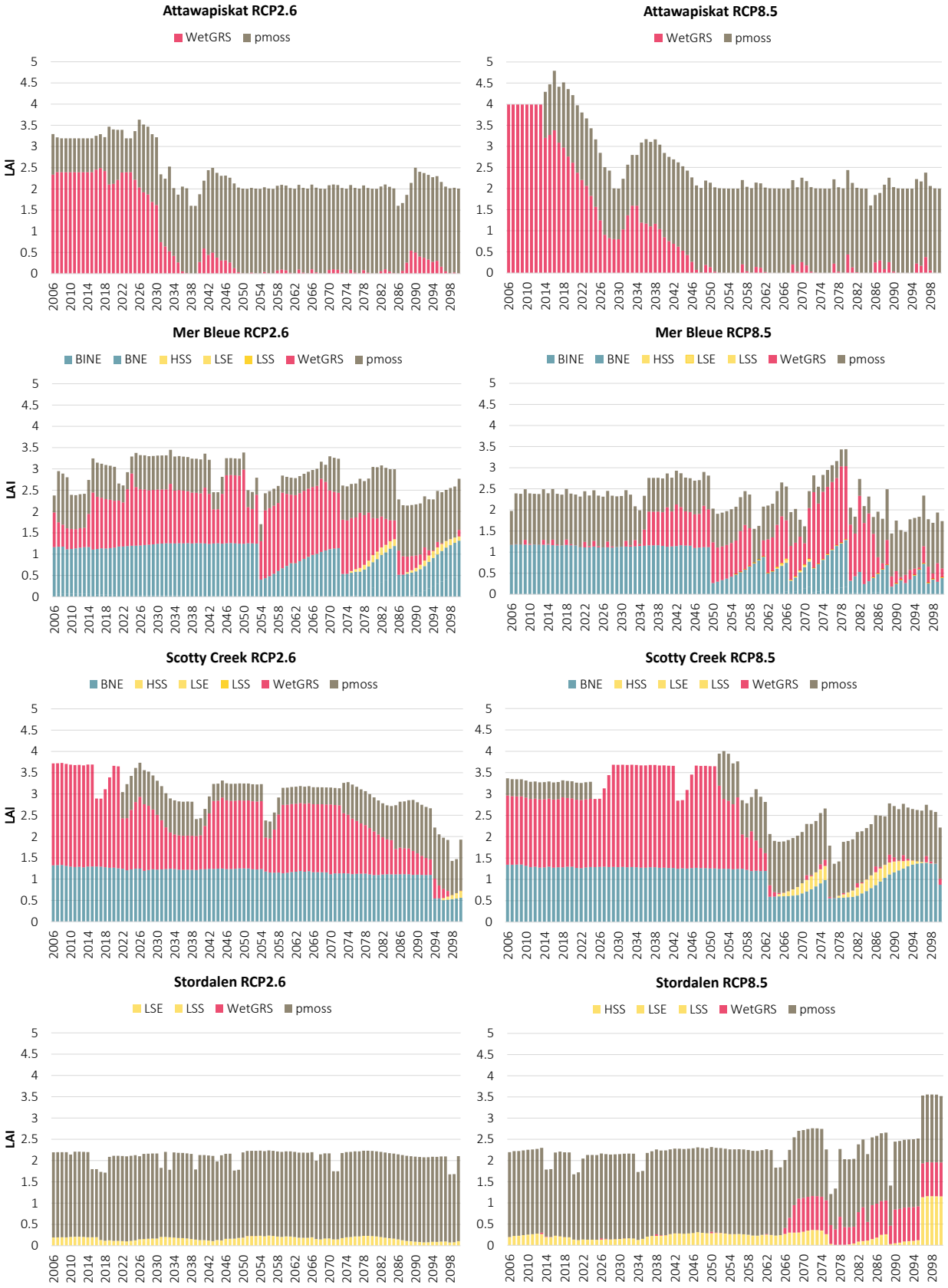

Figure 14. Leaf area index (LAI) per PFT between 2006-2100 under RCP2.6 (left) and RCP8.5 (right). LAI is expressed as leaf area per unit ground (m-2/m-2). The simulated PFTs are peatland mosses (pmoss), graminoids (WetGRS), high summergreen shrubs (HSS), low summergreen shrubs (LSS), low evergreen shrubs (LSE), and boreal needleleaved evergreen trees (BINE and BNE). Each simulation ran from peat initiation until 2100, resulting in slightly different values by 2006 due to the variation within the model.

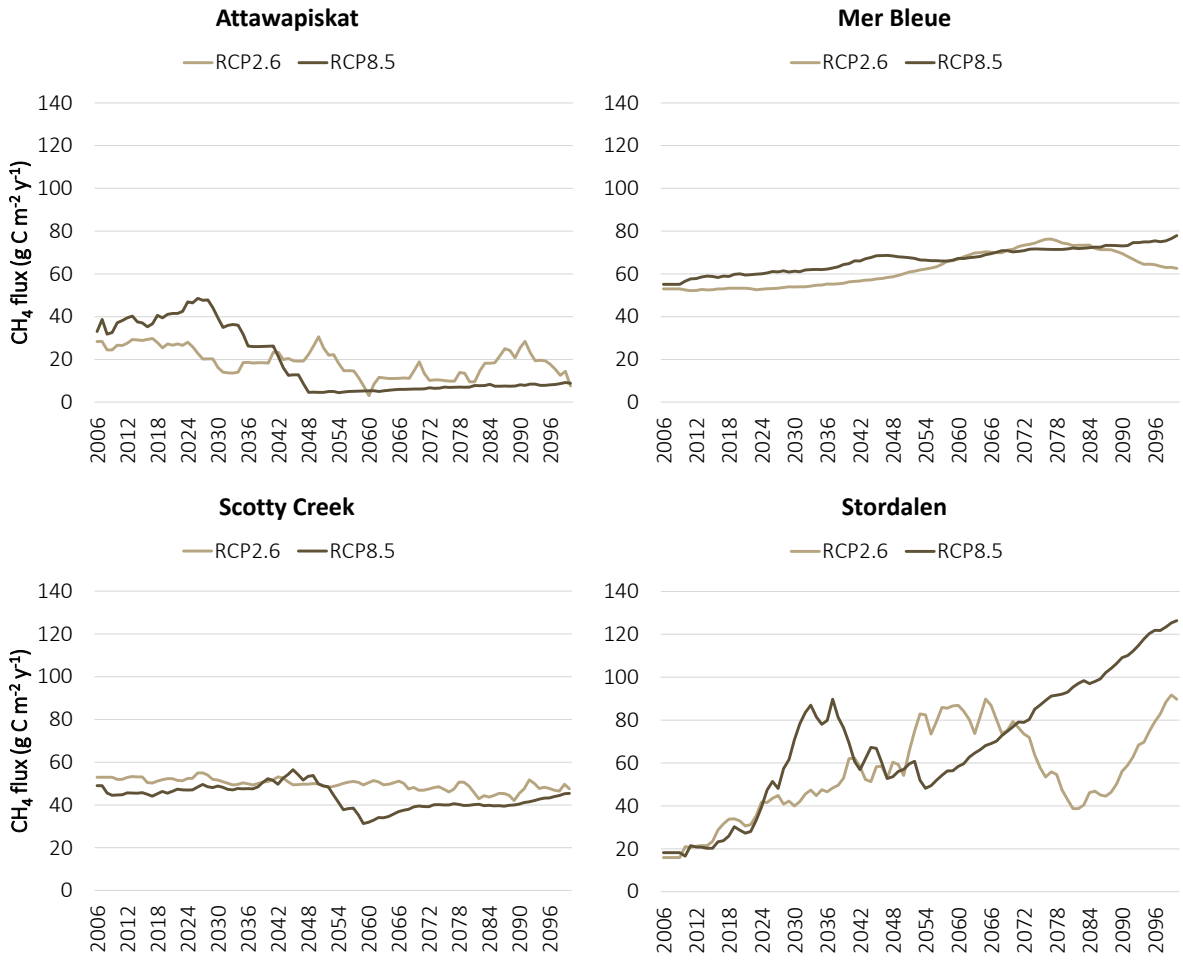

Figure 15. Modelled annual methane (CH_4) emissions between 2006-2100 under RCP2.6 (light brown) and RCP8.5 (dark brown). A moving average of 5 years was applied to smooth the data. Each simulation ran from peat initiation until 2100, resulting in slightly different values by 2006 due to the variation within the model.

4.5 Analysis of climatic controls

The findings from the linear regression analysis display the relationships between the response of atmospheric CO_2 concentrations, temperature, and precipitation individually assessed against the composite effects on NEP, CH_4, GPP, and R_{eco}. When exploring the impact of each forcing on carbon fluxes, it becomes important to consider the anticipated changes in each forcing. Over the period from 2000 to 2100, atmospheric CO_2 levels and temperature exhibited consistent increases across all sites. In contrast, projections indicated no noticeable change in precipitation at Scotty Creek, with minor increases projected in Mer Bleue and Attawapiskat, and the most substantial increase observed in Stordalen.

Figure 16 demonstrates a weak association in modelled NEP when influenced solely by precipitation and atmospheric CO_2 concentrations. The modelled NEP was primarily associated with the direct and indirect effects of the projected temperature change, with varying response among the sites (Fig. 16). The strongest relationship was observed in Attawapiskat, followed by Stordalen.

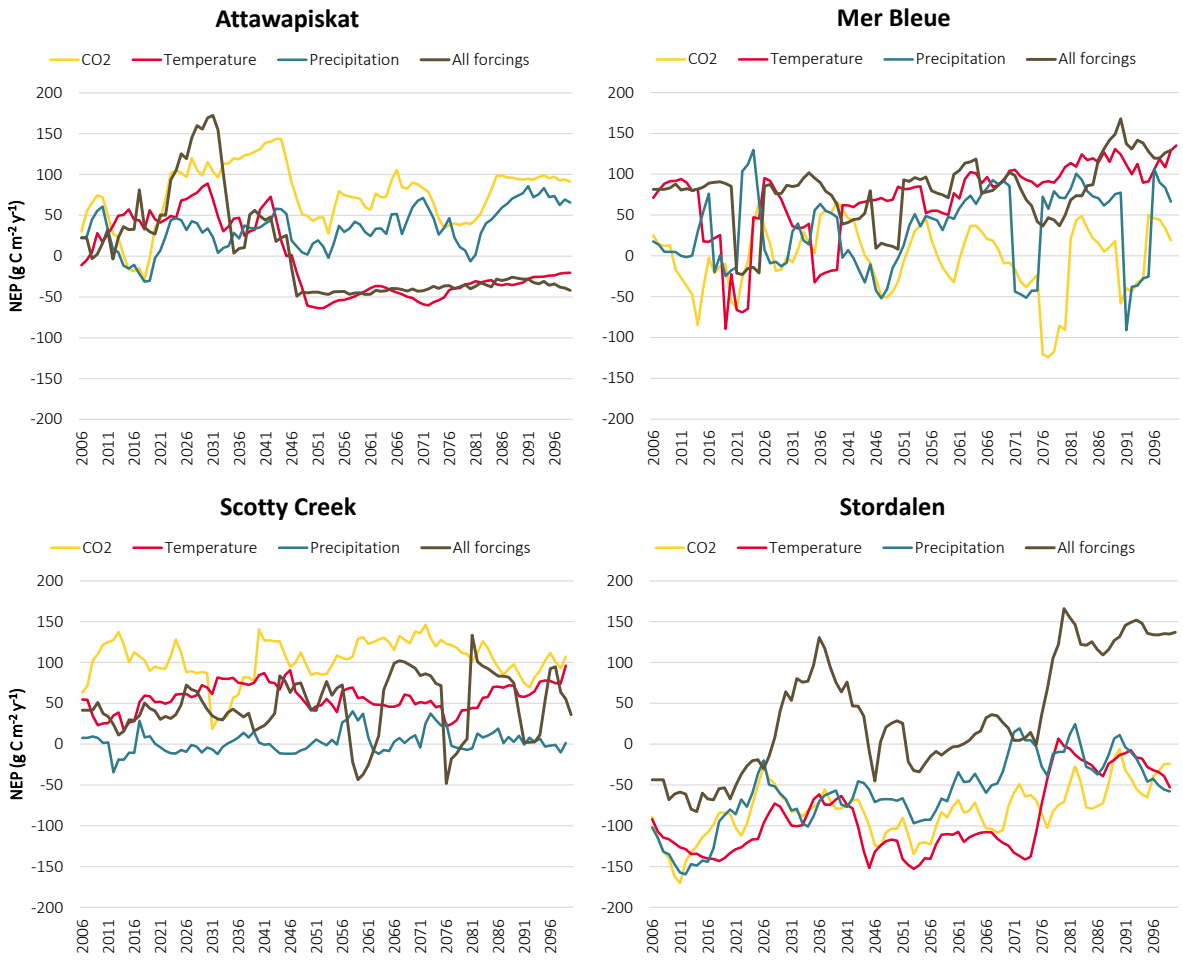

Fig 16. Modelled net ecosystem productivity (NEP) between 2006 and 2100 when forced only with projected atmospheric carbon dioxide levels (yellow), temperature (red), precipitation (blue), as well as all three forcings combined (black). A moving average of 5 years has been applied to smoothen the data.

Time series of the response of GPP and R_{eco} to different forcings are provided as supplementary material in Appendix A and B. Temperature appeared to influence the modelled GPP across all sites, whereas precipitation has a minor effect (Appendix A). Similarly to the observed pattern in NEP, atmospheric CO_2 concentrations generally had a low influence on GPP. Similarly, modelled R_{eco} demonstrated a weak association when influenced solely by precipitation and was found to be most closely related to temperature, although the response of the single forcing agents differed from the NEP with combined forcings (Appendix B). Modelled CH_4 emissions were however closely related to future temperature projections across all sites, while the direct and indirect effects of precipitation and atmospheric CO_2 concentrations had a minor influence (Fig. 17).

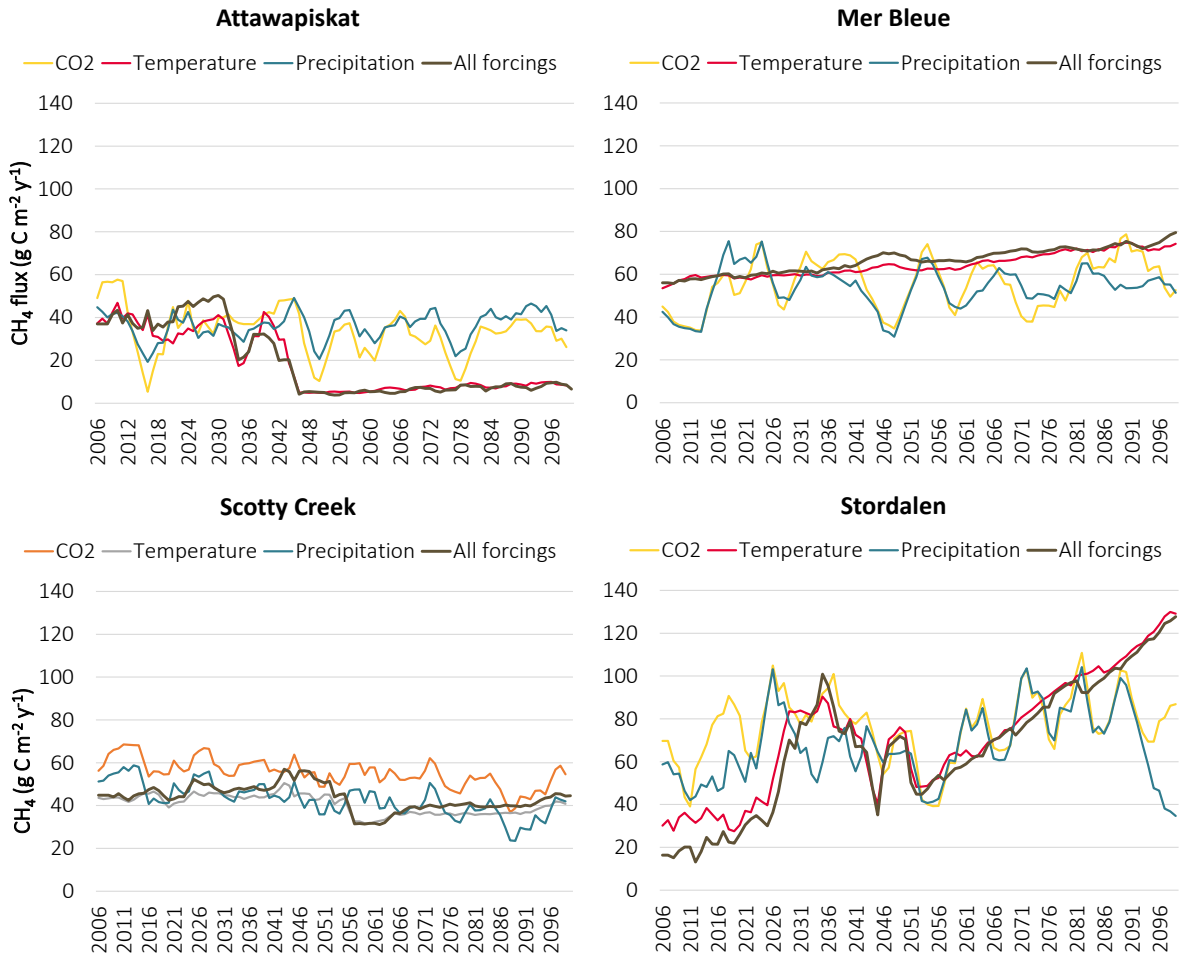

Fig 17. Modelled methane (CH_4) between 2006 and 2100 when forced only with projected atmospheric carbon dioxide content (yellow), temperature (red), precipitation (blue), as well as all three forcings combined (black). A moving average of 5 years has been applied to smoothen the data.

Although the modelled NEP and CH_4 emissions were mainly associated with temperature, the level of uncertainties in the regression analysis differs between the sites. RMSE, R^2, and regression slope of each factorial experiments are available in Appendix C. In the regression analysis of modelled NEP, the highest R^2 and regression slope were observed in Attawapiskat and Stordalen, indicating the strongest relationships (Appendix C). A robust relationship of CH_4 emissions forced with temperature was evident across all sites, with RMSE ranging between 1.9 and 5.1, indicating a high level of agreement (Appendix C). The regression analysis for R_{eco} and GPP produced high RMSE and low R^2 across all sites (Appendix C). The influence of atmospheric CO_2 concentrations on GPP, and subsequently NEP, is low across all sites, but the R^2 in Stordalen suggest that this peatland exhibited a greater sensitivity to changes in atmospheric CO_2 concentrations than the other sites (Appendix C). The regression analysis of NEP and GPP displayed a particularly low relationship with all climatic factors in Scotty Creek and Mer Bleue.

5. Discussion

5.1 Climatic controls on carbon fluxes

The high relationship observed between CH_4 emissions and temperature aligns with expectations, as increasing CH_4 emissions are attributed to heightened microbial respiration driven by temperature increments (Zhang et al., 2017). Additionally, the indirect effects of a warming climate can control CH_4 emissions through their effect on permafrost thaw and variations in WTP, contribute to the overall influence of temperature on CH_4 emissions **(**Abdalla et al., 2016). The weak relationships of the linear regression analyses suggest that the climatic factors may not directly regulate the temporal dynamics of GPP, R_{eco}, and NEP. The analysis does also not incorporate factors that indirectly influences the carbon dynamics, such as fire disturbances, which contributes to lowering of carbon sink capacities. Still, the relationship observed between R_{eco} and temperature is in line with expectations, as microbial activity and respiration is boosted in response to increasing temperatures. The anticipated CO_2 fertilization effect on GPP, which has the potential to increase primary production in less productive environments, is not evident in the results. The CO_2 fertilization effect boosts productivity when the peatland is not limited by moisture, temperature, or radiation, and it is possible that the influence of CO_2 is more prominent when combined with the other forcings. Neither is a strong relationship between temperature and GPP, where peatland net productivity is enhanced by warming (Wu & Roulet, 2014). The low agreement between NEP and the climate controls in Scotty Creek and Mer Bleue are partially due to the low agreement with GPP and the climate controls at these sites. However, the modelled GPP is also affected by indirect effects of the climate forcings, such as WTP and vegetation composition, and the modelled NEP is influenced by an interplay of multiple factors, such as vegetation establishment and fire disturbance that were not included in the analysis of climatic controls.

5.2 Future fate of northern peatlands

The four peatlands modelled in this project do not fully represent all northern peatlands across the northern hemisphere, but they provide an insight how carbon dynamics in subarctic and temperate peatlands in Europe and Canada could change under future climate scenarios. Existing regional modelling studies incorporate all crucial northern peatland regions, including the RFE and WSL that were not included in the scope of this project. Instead, the selected peatlands used to model future peatland carbon stocks and fluxes within this project contributes to the existing regional modelling studies by incorporating peatland dynamics at a more local scale.

5.2.1 Carbon stocks

The findings indicate a reduction in carbon stocks across all sites apart from Stordalen, where the existing modest carbon pool is anticipated to experience a marginal increase under both forcing scenarios (Fig. 8). Attawapiskat exhibits the most substantial decrease, significantly diminishing in size to the extent that it becomes nearly comparable in magnitude to the Mer Bleue site. Consequently, due to the pronounced reduction in Attawapiskat's carbon pool, Scotty Creek emerges as the largest carbon reservoir by the year 2100. Noteworthy

observations within the studied sites include the resilience of Scotty Creek under the RCP2.6 scenario, with carbon stocks remaining stable. Additionally, Mer Bleue's carbon stocks have displayed slight fluctuations over its historical trajectory, with carbon stocks increasing and subsequently decreasing when analyzing the four 50-year averages between 1900-2100. The low emission scenario results in changes in carbon stocks that are aligned with previous fluctuations, which could indicate a resilience. If global warming were to continue in line with the projections under RCP2.6, northern peatlands could maintain their carbon stock capacity. The relatively lower greenhouse gas emissions scenario outlined in RCP2.6 suggests a pathway that could mitigate the acceleration of climate change, potentially allowing these peatlands to sustain their current carbon storage levels. Furthermore, the carbon stock in Stordalen exhibits a more pronounced increase under RCP8.5, and most sites display a pattern with a slight increase in carbon stocks under RCP8.5 in the first half of the century followed by a rapid decrease. This trend aligns with previous model results where shifts in carbon sink capacities have started to occur by 2050 (Chaudhary et al., 2017a; 2020; Rafat et al., 2021).

5.2.2 Net ecosystem productivity and its components

The CRU data evaluation indicated historically low simulated temperatures, which potentially could have restricted GPP in these subarctic ecosystems where temperature often is a limiting factor. These factors could collectively have contributed to the overestimation in annual NEP observed across the sites, which results in a lower modelled carbon sink capacity. The results indicate that all Canadian sites could shift into carbon sources before 2100 already under a low emission scenario (RCP2.6), contrary to regional modelling studies that project all sites to remain as carbon sinks or carbon neutral under low and intermediate RCP scenarios (Chaudhary et al., 2022; Qiu et al., 2022). However, considering the underestimation of annual carbon sink capacity compared to historical observations, analyzing the trend of projected NEP is more informative. No apparent trend in NEP was observed in Attawapiskat, Scotty Creek, or Stordalen under RCP2.6, which indicates a resilience to climate change and continued role as carbon sinks (Fig. 9). If saturated soil conditions persist, peatlands will continue to sequester carbon dioxide from the atmosphere as decomposition is restricted by the waterlogged conditions (Holmes et al., 2022). Conversely, a trend of increasing NEP is observed at the temperate site Mer Bleue, even though water table become shallower. The temperate site is however susceptible to fire disturbance, being located in a warmer, temperate region compared to the other sites. This indicates a vulnerability of the carbon sink capacity, which potentially could be reduced even under global warming under RCP2.6 by 2100.

Under the high emission scenario (RCP8.5), both Stordalen and Mer Bleue are vulnerable to reduce their carbon sink capacity by 2100, possibly even shifting into carbon neutral or carbon source (Fig. 9). Although the magnitude of the annual NEP is uncertain, this aligns with existing studies projecting peatlands in Scandinavia, HBL, and eastern Canada to decrease their carbon sink capacity or shift into carbon sources by 2100 under RCP8.5 as boosted respiration rates exceed net productivity (Chaudhary et al., 2017a; 2020; 2022; McLaughlin & Packalen, 2021; Qiu et al., 2022). In contrast, NEP remains stable in Scotty Creek and decreases in Attawapiskat under RCP8.5, indicating robust carbon sink capacities in these sites. Existing studies differ in their projections of Western Canada and HBL where Scotty Creek and Attawapiskat are located, some projecting stronger carbon sinks and others

a shift into carbon sources (Chaudhary et al., 2017a; 2022; Qiu et al., 2022). Local modelling studies do however confirm potential shifts into significant carbon sources, since decomposition rates are projected to dominate net productivity in response to increasing temperatures (Helbig et al., 2017; Rafat et al., 2021). The insights from this study add new understanding to how these Canadian subarctic sites might respond in a future climate. Increasing sink capacities are usually attributed to prolonged growing seasons at high latitudes, thereby increasing NPP in areas that are not water limited, which aligns with the results in Attawapiskat. (Loisel et al., 2016).

It is important to acknowledge that the NEP results presented in this study are modeled considering natural disturbances and vegetation establishment patterns, which exert an influence particularly under the RCP8.5 scenario where fire disturbances become more frequent in the prolonged dry and warm conditions (Fig. 11). These disturbances can profoundly impact peatland carbon dynamics by altering vegetation composition, and thereby accelerating decomposition, and releasing stored carbon into the atmosphere. Without these natural dynamics, the trend of the computed net difference between GPP and R_{eco} provides conflicting information on the future of these peatlands (Fig. 10). Instead of being resilient to changes in NEP under RCP2.6, a decrease in sink capacity is observed for all sites except Mer Bleue when vegetation establishment and fire disturbance is disregarded. Additionally, the carbon sink capacities in Stordalen and Mer Bleue increases, instead of decreases, when analysing the net difference between GPP and R_{eco}.

5.2.3 Methane emissions

The results indicate a rapid thawing of permafrost with a potential depletion under RCP8.5 resulting in a deepening of ALD across the subarctic sites, which confirms findings from previous modelling studies (Fig. 12a; Fig. 12b) (Chaudhary et al 2017a; 2017b; 2020; Holmes et al., 2022). Despite being overestimated, the modelled trend of CH_4 emissions to changing climate conditions offers valuable insights into potential future trends. In Stordalen and Mer Bleue, CH_4 emissions increase steadily throughout the century under both scenarios, with higher fluxes observed under RCP8.5 (Fig. 15). This aligns well with existing modelling studies which project substantial increases in CH_4 emissions from northern peatlands under RCP8.5, while responses to RCP2.6 vary, with some models projecting slight increases and others stable emissions over the century (Qiu et al., 2022). The increase in CH_4 emissions is driven by warmer soil temperatures promoting microbial respiration, coupled with the availability of previously frozen organic matter for decomposition as permafrost thaws and the hydrological conditions shift into more unsaturated, anaerobic conditions. The modelled decrease in soil ice fraction, and subsequent increase water content in the soil, confirms these findings. Interestingly, in Scotty Creek and Attawapiskat under RCP8.5, CH_4 emissions rapidly decline and stabilize around mid-century, coinciding with soil ice depletion and an increase in ALD. Previous modelling conducted in the HBL have suggested that high emission scenarios could lead to peat drying and decreased CH_4 emissions due to altered hydrological conditions with increasing temperature and evapotranspiration but unchanged precipitation rates (Abdalla et al., 2016; McLaughlin & Packalen, 2021). This is a plausible explanation for the observed trend in CH_4 emissions in Scotty Creek. The presence of unsaturated soil conditions, coupled with deepening of water tables, shift in vegetation from

graminoids to mosses, and rising air and soil temperatures, indicate drying of peat which decrease CH_4 emissions (Fig. 13). Conversely, saturated soil conditions typically promote CH_4 production and transport, as they create anaerobic conditions favourable for CH_4 production, and encourage the growth of vascular plants with efficient CH_4 transportation capabilities (Abdalla et al., 2016). However, in Attawapiskat, vegetation shifts from graminoids to mosses which indicates a potential drying, while the observed WTP remain at saturated conditions and do not align with expected CH_4 emissions (Fig. 13). The reduced CH_4 emissions could be attributed to the shift in vegetation, as graminoids are related to higher CH_4 production and transport. However, further investigation is required to fully understand the dynamics driving CH_4 emissions at this site, as continuously waterlogged conditions promote graminoids and increased CH_4 emissions.

5.3 Limitations

5.3.1 Climate data

The assessment of historical CRU data indicates that simulated historical temperatures are lower than observed values across most sites. The colder historical data likely contributed to the overestimations in NEP due to prohibiting net productivity in the unproductive subarctic ecosystems. While precipitation also deviates from observations, it is not expected to have influenced the results as significantly as temperature. Although it is probable that Attawapiskat, where observed climate data is unavailable, aligns with the other sites, the absence of observed multi-year climate data remains a limitation. The spatial availability of observed climate data further restricts the evaluation, particularly considering that the nearest climate stations to Attawapiskat and Scotty Creek are situated 100 km and 60 km away, respectively. Consequently, these observations may not fully represent the local climate at the sites. It is equally important to acknowledge that the spatial resolution of the CRU data at 0.5° does not capture site-specific climate characteristics, but rather represents regional averages. Additionally, climate projections are susceptible to errors, primarily due to their 0.5° spatial resolution and the challenge of accurately representing local climates within each grid. However, the IPSL-CM5A-LR projections from the ISIMIP repository used in this study are bias-adjusted to observation data on daily time steps, mitigating potential errors and resulting in a dataset with a smoother transition between historical data and future projections. Nevertheless, a lag persists between historical and future climate data, as two datasets were not adequately corrected and should have undergone additional bias correction.

A single simulation using corrected historical climate data for Stordalen revealed elevated CH_4 emissions between 1900 and 2000. This increase can be attributed to variations in vegetation composition and hydrological conditions, with the presence of graminoids and shallower WTP during in the corrected climate simulation, contrasting with dominance by mosses in uncorrected climate simulation. Additionally, the historical NEP in Stordalen was higher, indicating a lower carbon sink compared to the uncorrected climate simulation. Both CH_4 emissions and NEP exceeded the observed range documented in literature.

5.3.2 Evaluation data

The low data availability, particularly in remote regions such as northern Canada, impedes comprehensive evaluations of carbon stocks and fluxes. The lack of evaluation data is largest in Canada, where vast parts of the country is off the grid, which limits the collection of continuous data. However, understanding the dynamics of these sub-arctic peatlands is particularly important in order to assess their response to climate change due to the vast areas they cover, their large carbon stocks, and the unexploited landscape. Existing datasets from reputable networks (e.g., ABCflux, FluxNet, AmeriFlux, ICOS) exhibit significant data gaps, at times including multiple months of missing information for each available year. Even though gap-filling is possible in situation where few data is missing, it was not possible to accurately evaluate annual carbon fluxes when multiple months are missing. The temporal and spatial limitations, combined with the truncated duration of available data, complicates the evaluation of the model results of historical carbon fluxes. The scarcity of comprehensive data on variables like GPP and R_{eco} further exacerbates the evaluation of the results. Additionally, evaluating single-year results is challenging due to the annual model variation, and longer averages or trends should ideally be considered if there is longer time series of observations to support this.

5.4 Future studies

Moving forward, additional steps are crucial to refine the accuracy of the simulations and provide more reliable insights into the potential outcomes under different future forcing scenarios. An optimal approach involves including corrected historical climate data, or even observed historical climate datasets when available, although this is challenging for sites observational data is limited. Further evaluation with observations from literature and datasets is also essential to accurate evaluate the performance of the model on site-specific peatlands, and further simulations incorporating other local peatlands should be considered. Equally crucial is the use of model parametrization to accurately tune the model settings to adapt the model to the studied peatland, which was not included in the scope of this project. Additionally, it is important to incorporate climate projections from more GCM as well as using a full range of climate projection scenarios under CMIP5 or CMIP6 to fully assess the fate of peatlands in LPJ-GUESS.

6. Conclusions

In this study, the LPJ-GUESS model was used to analyse historical and future carbon dynamics of northern peatlands. Evaluation against observations revealed a trend of more positive net ecosystem productivity (NEP) and methane (CH_4) emissions compared to observations. This indicates that the model produced higher carbon emissions of CO_2 and CH_4 from the studied peatlands which lead to uncertainties in the future carbon balance assessments. The overestimation of carbon fluxes in comparison to local observations can be attributed to the quality of climate data and the lack of local model parameterization. Despite these limitations, the trends in the modelled carbon stocks and fluxes provide valuable insights into peatland dynamics and potential responses to climate change. The results

suggests that peatlands could maintain their carbon sink capacity under the low emission scenario RCP2.6, potentially mitigating the impacts of climate change. However, under the high emission scenario RCP8.5, anticipated changes in peatland carbon stocks across Canadian sites indicate a reduction, with Attawapiskat projected to be particularly vulnerable to carbon stock losses. The projected trends in NEP indicate that Stordalen and Mer Bleue are vulnerable to transition into annual carbon sources, accompanied by an increase in CH_4 emissions, underscoring the importance of reducing greenhouse gas emissions. Nevertheless, Scotty Creek and Attawapiskat stand out as exceptions, projected to maintain, or even increase their carbon sink capacities while reducing peatland CH4 emissions, indicating a potential resilience to climate change. Temperature emerges as a key driver for future NEP and CH_4 emissions. Moving forward, it is imperative to incorporate bias-corrected historical data and continue the evaluation with observations to enhance the accuracy of the projections and enhance our understanding of local peatland carbon dynamics.

References

Abdalla, M., Hastings, A., Truu, J., Espenberg, M., Mander, Ü., & Smith, P. (2016). Emissions of methane from northern peatlands: a review of management impacts and implications for future management options. *Ecology and Evolution 6*(19), 7080-7102. 10.1002/ece3.2469

Brown, R. J. E. (1973). Permafrost: distribution and relation to environmental factors in the Hudson Bay lowland. *Symposium on the Physical Environment of the Hudson Bay Lowland*, 35–68. https://nrc-publications.canada.ca/eng/view/ft/?id=de2095a3-557b-4bd5-8474-5a00f2a398b6

Bunbury, J., Finkelstein, S., & Bollmann, J. (2012). Holocene hydro-climatic change and effects on carbon accumulation inferred from a peat bog in the Attawapiskat River watershed, Hudson Bay Lowlands, Canada. *Quaternary Research, 78*(2), 275-284. https://doi.org/https://doi.org/10.1016/j.yqres.2012.05.013

Canadian Centre for Climate Services [CCCS]. (n.d.). *Daily climate data* [Data set]. Government of Canada. Retrieved September 18, 2023 from https://climate-change.canada.ca/climate-data/#/daily-climate-data

Chartrand, P. G., Sonnentag, O., Sanderson, N. K., & Garneau, M. (2023). Recent peat and carbon accumulation on changing permafrost landforms along the Mackenzie River valley, Northwest Territories, Canada. *Environmental Research Letters, 18*(9), 095002. https://doi-org.ludwig.lub.lu.se/10.1088/1748-9326/ace9ed

Chaudhary, N., Miller, P. A., & Smith, B. (2017a). Modelling past, present and future peatland carbon accumulation across the pan-Arctic region. *Biogeosciences, 14*(18), 4023–4044. https://doi.org/10.5194/bg-14-4023-2017

Chaudhary, N., Miller, P. A., & Smith, B. (2017b). Modelling Holocene peatland dynamics with an individual-based dynamic vegetation model. *Biogeosciences, 14*(10), 2571–2596. https://doi.org/10.5194/bg-14-2571-2017

Chaudhary, N., Westermann, S., Lamba, S., Shurpali, N., Sannel, A. B. K., Schurgers, G., Miller, P. A., & Smith, B. (2020). Modelling past and future peatland carbon dynamics across the pan-Arctic. *Global Change Biology, 26*(7), 4119–4133. https://doi-org.ludwig.lub.lu.se/10.1111/gcb.15099

Chaudhary, N., Zhang, W., Lamba, S., & Westermann, S. (2022). Modeling Pan-Arctic Peatland Carbon Dynamics Under Alternative Warming Scenarios. *Geophysical Research Letters, 49*(10). https://doi-org.ludwig.lub.lu.se/10.1029/2021GL095276

European Environment Agency [EEA]. (2019). *Trends in atmospheric concentrations of CO2 (ppm), CH4 (ppb) and N2O (ppb), between 1800 and 2017* [Data set]. Retrieved September 21, 223 from https://www.eea.europa.eu/data-and-maps/daviz/atmospheric-concentration-of-Carbon-dioxide-5.

Finlayson, C.M., & Milton, G.R. (2018). Peatlands. In: C, Finlayson, G Milton, R. Prentice, & N. Davidson (Eds.), *The Wetland Book.* Springer, Dordrecht. https://doi.org/10.1007/978-94-007-4001-3_202

Flato, G., Marotzke, J., Abiodun, B., Braconnot, P., Chou, S.C., Collins, W., Cox, P., Driouech, F., Emori, S., Eyring, V., Forest, C., Gleckler, P., Guilyardi, E., Jakob, C., Kattsov, V., Reason, C., & Rummukainen, M. (2013). Evaluation of Climate Models. In Stocker, T.F., Qin, D., Plattner, Q.-K., Tignor, M., Allen, S.K., Boschung, J., Nauels, A., Xia, Y., Bex, V., & Midgley, P.M, (Eds.), *Climate Change 2013: The Physical Science Basis. Contribution of Working Group I to the Fifth Assessment Report of the Intergovernmental Panel on Climate Change (pp. 741-866)*. Cambridge University Press, Cambridge, UK and New York, USA.

Frolking, S., Roulet, N. T., Tuittila, E., Bubier, J. L., Quillet, A., Talbot, J., & Richard, P. J. H. (2010). A new model of Holocene peatland net primary production, decomposition, water balance, and peat accumulation. *Earth System Dynamics*, 1(1), 1–21. https://doi-org.ludwig.lub.lu.se/10.5194/esd-1-1-2010

Frolking, S., Talbot, J., Jones, M. C., Treat C. C., Kauffman, J.B., Tuittila, E-S., & Roulet, N. (2011) Peatlands in the Earth's 21st century climate system. *Environmental Reviews*. 19(NA): 371-396. https://doi.org/10.1139/a11-014

Harris, L. I., Richardson, K., Bona, K. A., Davidson, S. J., Finkelstein, S. A., Garneau, M., McLaughlin, J., Nwaishi, F., Olefeldt, D., Packalen, M., Roulet, N.T., Southee, F. M., Strack, M., Webster, K. L., Wilkinson, S. L., & Ray, J. C. (2021). The essential carbon service provided by northern peatlands. *Frontiers in Ecology and the Environment 20*(4), 222-230. https://doi.org/10.1002/fee.2437

Haynes, K. M., Connon, R. F., & Quinton, W. L. (2019). Hydrometeorological measurements in peatland-dominated, discontinuous permafrost at Scotty Creek, Northwest Territories, Canada. *Geoscience Data Journal, 6*(2), 85-96. https://doi.org/10.1002/gdj3.69

Helbig, M., Chasmer, L.E., Desai, A.R., Kljun, N., Quinton, W.L., & Sonnentag, O. (2017). Direct and indirect climate change effects on carbon dioxide fluxes in a thawing boreal forest–wetland landscape. *Global Change Biology, 23*(8), 3231-3248. https://doi.org/10.1111/gcb.13638

Helbig, M., Humphreys, E. R., & Todd, A. (2019). Contrasting temperature sensitivity of CO_2 exchange in peatlands of the Hudson Bay Lowlands, Canada. *Journal of Geophysical Research: Biogeosciences, 124*(7), 2126–2143. https://doi-org.ludwig.lub.lu.se/10.1029/2019JG005090

Holmes, M. E., Crill, P. M., Burnett, W. C., McCalley, C. K., Wilson, R. M., Frolking, S., Chang, K.-Y., Riley, W. J., Varner, R. K., Hodgkins, S. B., Coordinators, I. P., Team, I. F., McNichol, A. P., Saleska, S. R., Rich, V. I., & Chanton, J. P. (2022). Carbon accumulation, flux, and fate in Stordalen Mire, a permafrost peatland in transition. *Global Biogeochemical Cycles*, 36(1), e2021GB007113. https://doi-org.ludwig.lub.lu.se/10.1029/2021GB007113

Integrated Carbon Observation Systems [ICOS]. (n.d.). *Networks and Measurements - Abisko Stordalen*. ICOS Sweden. Retrieved September 4, 2023, from https://www.icos-sweden.se/abisko-stordalen

International Institute for Applied Systems Analysis [IIASA]. (2009). *Representative Concentration Pathways Database* (Version 2.0) [Data set]. RCP Database. (Version 2.0.5). Retrieved September 20, 2023, from http://tntcat.iiasa.ac.at/RcpDb/

IPCC. (2023). Section 3: Long-Term Climate and Development Futures. In H. Lee and J. Romero (Eds.), *Climate Change 2023: Synthesis Report. Contribution of Working Groups I, II and III to the Sixth Assessment Report of the Intergovernmental Panel on Climate Change* (35-115*)*. IPCC. Geneva, Switzerland, doi: 10.59327/IPCC/AR6-9789291691647

Johansson, T., Malmer, N., Crill, P. M., Friborg, T., Åkerman, J. H., Mastepanoc, M., & Christensen, T. R. (2006). Decadal vegetation changes in a northern peatland, greenhouse gas fluxes and net radiative forcing. *Global Change Biology*, 12, 2352–2369. https://doi.org/10.1111/j.1365-2486.2006.01267.x

Johansson, M., Åkerman, J., Keuper, F., Christensen, T., Lantuit, H., & Callaghan, T. (2011). Past and present permafrost temperatures in the Abisko area: redrilling of boreholes. *Ambio, 40*(6), 558–565. https://doi.org/10.1007/s13280-011-0163-3

Łakomiec, P., Holst, J., Friborg, T., Crill, P., Rakos, N., Kljun, N., Olsson, P.-O., Eklundh, L., Persson, A., & Rinne, J. (2021). Field-scale CH_4 emission at a subarctic mire with heterogeneous permafrost thaw status, *Biogeosciences, 18*(20), 5811–5830. https://doi.org/10.5194/bg-18-5811-2021

Lange, S., & Büchner, M. (2017). *ISIMIP2b bias-adjusted atmospheric climate input data* (Version 1.0) [Data set]. ISIMIP Repository. https://doi.org/10.48364/ISIMIP.208515

McLaughlin, J. W., & Packalen, M. S. (2021). Peat Carbon Vulnerability to Projected Climate Warming in the Hudson Bay Lowlands, Canada: A Decision Support Tool for Land Use Planning

in Peatland Dominated Landscapes. *Frontiers in Earth Science, 9*. https://doi.org/10.3389/feart.2021.650662

Miller, P. A., Giesecke, T., Hickler, T., Bradshaw, R. H. W., Smith, B., Seppä, H., Valdes, P. J., & Sykes, M. T. (2008). Exploring climatic and biotic controls on Holocene vegetation change in Fennoscandia. *Journal of Ecology, 96*(2), 247-259. https://doi.org/10.1111/j.1365-2745.2007.01342.x

Miller, P. A. & Smith, B. (2012). Modelling Tundra Vegetation Response to Recent Arctic Warming. *Ambio, 41, 281–291,* doi:10.1007/s13280-012-0306-1

Mitchell, T. D., & Jones, P.D. (2005). An improved method of constructing a database of monthly climate observations and associated high-resolution grids. *International Journal of Climatology, 25*(6) 693-712. https://doi-org.ludwig.lub.lu.se/10.1002/joc.1181

O'Brien, E., & Nolan, P. (2023). TRANSLATE: standardized climate projections for Ireland. *Frontiers in Climate 5*. 10.3389/fclim.2023.1166828

Obu, J., Westermann, S., Barboux, C., Bartsch, A., Delaloye, R., Grosse, G., Heim, B., Hugelius, G., Irrgang, A., Kääb, A.M., Kroisleitner, C., Matthes, H., Nitze, I., Pellet, C., Seifert, F.M., Strozzi, T., Wegmüller, U., Wieczorek, M., Wiesmann, A. (2021). *Permafrost extent for the Northern Hemisphere* (Ver. 3.0) [Data set]. ESA Permafrost Climate Change Initiative. NERC EDS Centre for Environmental Data Analysis. doi:10.5285/6e2091cb0c8b4106921b63cd5357c97c.

O'Neill, B., van Aalst, M., Zaiton Ibrahim, Z., Berrang Ford, L., Bhadwal, S., Buhaug, H., Diaz, D., Frieler, K., Garschagen, M., Magnan, A., Midgley, G., Mirzabaev, A., Thomas, A., & Warren, R. (2022). Key Risks Across Sectors and Regions. In H.-O. Pörtner, D.C. Roberts, M. Tignor, E.S. Poloczanska, K. Mintenbeck, A. Alegría, M. Craig, S. Langsdorf, S. Löschke, V. Möller, A. Okem, & B. Rama (Eds.), *Climate Change 2022: Impacts, Adaptation and Vulnerability. Contribution of Working Group II to the Sixth Assessment Report of the Intergovernmental Panel on Climate Change* (2411–2538). Cambridge University Press, Cambridge, UK and New York, NY, USA, doi:10.1017/9781009325844.025

Packalen, M., Finkelstein, S., & McLaughlin, J. (2014). Carbon storage and potential methane production in the Hudson Bay Lowlands since mid-Holocene peat initiation. *Nature Communications 5*(1), 4078. https://doi.org/10.1038/ncomms5078

Packalen, M. S., Finkelstein, S. A., & McLaughlin, J. W. (2016). Climate and peat type in relation to spatial variation of the peatland carbon mass in the Hudson Bay Lowlands, Canada. *Journal of Geophysical Research: Biogeosciences, 121*(4), 1104–1117, doi:10.1002/2015JG002938.

Parmesan, C., Morecroft, M.D., Trisurat Y., Adrian, R., Anshari, G.Z., Arneth, A., Gao, Q., Gonzalez, P., Harris, R., Price, J., Stevens, N., & Talukdarr, G.H. (2022). Terrestrial and Freshwater Ecosystems and Their Services. In H.-O. Pörtner, D.C. Roberts, M. Tignor, E.S. Poloczanska, K. Mintenbeck, A. Alegría, M. Craig, S. Langsdorf, S. Löschke, V. Möller, A. Okem, B. Rama (Eds.), *Climate Change 2022: Impacts, Adaptation and Vulnerability. Contribution of Working Group II to the Sixth Assessment Report of the Intergovernmental Panel on Climate Change* (197–377) Cambridge University Press, Cambridge, UK and New York, NY, USA, doi:10.1017/9781009325844.004

Qiu, C., Ciais, P., Zhu, D., Guenet, B., Chang, J., Chaudhary, N., Kleinen, T., Li, X. Y., Müller, J., Xi, Y., Zhang, W., Ballantyne, A., Brewer, S. C., Brovkin, V., Charman, D. J., Gustafson, A., Gallego-Sala, A. V., Gasser, T., Holden, J., … Westermann, S. (2022). A strong mitigation scenario maintains climate neutrality of northern peatlands. *One Earth BECC: Biodiversity and Ecosystem Services in a Changing Climate MERGE: ModElling the Regional and Global Earth System ESSENCE: The e-Science Collaboration*, *5*(1), 86–97. https://doi-org.ludwig.lub.lu.se/10.1016/j.oneear.2021.12.008

Quinton, W. L., Hayashi, M., & Chasmer, L. E. (2011). Permafrost-thaw-induced land-cover change in the Canadian subarctic: implications for water resources. *Hydrological Processes, 25*(1), 152-158. https://doi-org.ludwig.lub.lu.se/10.1002/hyp.7894

Quinton, W., Berg, A., Braverman, M., Carpino, O., Chasmer, L., Connon, R., Craig, J., Devoie, E., Hayashi, M., Haynes, K., Olefeldt, D., Pietroniro, A., Rezanezhad, F., Schincariol, R., & Sonnentag, O. (2019). A synthesis of three decades of hydrological research at Scotty Creek, NWT, Canada. *Hydrology and Earth System Science 23*(4), 2015-2039. https://doi.org/10.5194/hess-23-2015-2019

Rantanen, M., Karpechko, A.Y., Lipponen, A., Nordling, K., Hyvärinen, O., Ruosteenoja, K., Vihma, T., & Laaksonen, A. (2022). The Arctic has warmed nearly four times faster than the globe since 1979. *Communications Earth & Environment 3*(1), 168. https://doi.org/10.1038/s43247-022-00498-3

Rinne, J., & ICOS Sweden (2021). *Ecosystem fluxes time series (ICOS Sweden), Abisko-Stordalen Palsa Bog, 2013-12-31–2014-12-31* [Data set]. Swedish National Network, https://hdl.handle.net/11676/ehlPSErCrubT1rn_8T9AhMkmn

Roulet, N. T., Lafleur, P. M., Richard, P. J. H., Moore, T. R., Humphreys, E. R., & Bubier, J. L. (2007). Contemporary carbon balance and late Holocene carbon accumulation in a northern peatland. *Global Change Biology 13*(2), 397-411. https://doi-org.ludwig.lub.lu.se/10.1111/j.1365-2486.2006.01292.x

Smith, B., Prentice, I. C., & Sykes, M. T. (2001). Representation of vegetation dynamics in the modelling of terrestrial ecosystems: comparing two contrasting approaches within European climate space. *Global Ecology and Biogeography, 10*(6), 621–637. https://doi.org/10.1046/j.1466-822X.2001.t01-1-00256.x

Sonnentag, O., Fouche, J., Helbig, M., Gosselin, G. H., Detto, M., Connon, R., Quinton, W., & Moore, T. (2020). A thawing boreal peat landscape along the southern limit of permafrost presently is carbon neutral. *Geophysical Research Abstracts, 22*, EGU General Assembly 2020. https://doi-org.ludwig.lub.lu.se/10.5194/egusphere-egu2020-6621

Sonnentag, O. & Quinton, W. (2021). *AmeriFlux BASE CA-SCB Scotty Creek Bog (*Ver. 2.5) [Data set]. AmeriFlux AMP. https://doi.org/10.17190/AMF/1498754

Stoffer, D., & Poison, N (2023). *ASTSA- Applied Statistical Time Series Analysis* (Ver. 2.0) [Data set]. https://dsstoffer.github.io/

Swedish Meteorological and Hydrological Institute [SMHI]. (n.d.). *Ladda ner meteorologiska observationer [Download meteorological observations]* [Data set]. Retrieved September 18, 2023 from https://www.smhi.se/data/meteorologi/ladda-ner-meteorologiska-observationer

Talbot, J., Pelletier, N., Olefeldt, D., Turetsky, M., Blodau, C., Sonnentag, O., & Quinton, W. (2017). The paleoecology, peat chemistry and carbon storage of a discontinuous permafrost peatland. *Geophysical Research Abstracts, 19.* EGU General Assembly 2017

Tang, J., Miller, P., Persson, A., Olefeldt, D., Pilesjö, P., Heliasz, M., Jackowicz-Korczynski, M., Yang, Z., Smith, B., Callaghan, T. V., & Christensen, T. R. (2015). Carbon budget estimation of a subarctic catchment using a dynamic ecosystem model at high spatial resolution. *Biogeosciences 12*(9), 2791-2808, 10.5194/bg-12-2791-2015

Taylor, K. E., Stouffer, R. J., & Meehl, G. A. (2012). An Overview of CMIP5 and the Experiment Design. *Bulletin of the American Meteorological Society, 93*(4), 485–498. https://doi.org/10.1175/BAMS-D-11-00094.1

Todd, A., & Humphreys, E. (2022). *AmeriFlux FLUXNET-1F CA-ARB Attawapiskat River Bog* (Ver. 3.5) [Data set]. AmeriFlux AMP. https://doi.org/10.17190/AMF/1902821

Virkkala, A.-M., Natali, S., Rogers, B. M., Watts, J. D., Savage, K., Connon, S. J., Mauritz-tozer, M. E., Schuur, E. A. G., Peter, D. L., Minions, C., Nojeim, J., Commane, R., Emmerton, C. A.,

Goeckede, M., Helbig, M., Holl, D., Iwata, H., Kobayashi, H., Kolari, P., … & Zyryanov, V. I. (2021). *The ABCflux Database: Arctic-Boreal CO2 Flux and Site Environmental Data, 1989-2020* (Ver. 1) [Data set]. ORNL Distributed Active Archive Center. https://doi.org/10.3334/ORNLDAAC/1934

Vitt, D.H. (2008). Peatlands. In S-E. Jørgensen, B. D. Fath, (Eds.), *Encyclopedia of* Ecology (2656-2664). Academic Press. https://doi.org/10.1016/B978-008045405-4.00318-9

Wania, R., Ross, I., & Prentice, I. C. (2009a) Integrating peatlands and permafrost into a dynamic global vegetation model: 1, Evaluation and sensitivity of physical land surface processes. *Global Biogeochemical cycles, 23*(3), doi:10.1029/2008gb003412

Wania, R., Ross, I., & Prentice, I. C. (2009b). Integrating peatlands and permafrost into a dynamic global vegetation model: 2, Evaluation and sensitivity of vegetation and carbon cycle processes. *Global Biogeochemical cycles, 23*(3), doi:10.1029/2008gb003413

Wania, R., Ross, I., & Prentice, I. C. (2010). Implementation and evaluation of a new methane model within a dynamic global vegetation model: LPJ-WHyMe v1.3.1. *Geoscientific Model Development, 3*(2), 565–584, doi:10.5194/gmd-3-565-2010

Wu, J., & Roulet, N. T. (2014). Climate change reduces the capacity of northern peatlands to absorb the atmospheric carbon dioxide: The different responses of bogs and fens. *Global Biogeochemical Cycles*, 28, 1005–1024, doi:10.1002/2014GB004845

Xu, J., Morris, P. J., Liu, J., & Holden, J. (2017). *PEATMAP: Refining estimates of global peatland distribution based on a meta-analysis* [Data set]. University of Leeds. https://doi.org/10.5518/252

Yu, Z., Beilman, D. W., & Jones, M. C. (2009). Sensitivity of Northern Peatland Carbon Dynamics to Holocene Climate Change. In A. J. Baird., L. R. Belyea, X. Comas, A. S. Reeve, & L. D. Slater (Eds), *Northern Peatlands* (Vol. 184). https://doi.org/10.1029/2008GM000822

Yu, Z. C. (2012). Northern peatland carbon stocks and dynamics; a review. *Biogeosciences*, *9*(10), 4071–4085. https://doi-org.ludwig.lub.lu.se/10.5194/bg-9-4071-2012

Zhang, W., Miller, P. A., Smith, B., Wania, R., Koenigk, T., & Doscher, R. (2013). Tundra Shrubification and Tree-line Advance Amplify Arctic Climate Warming: Results from an Individual-based Dynamic Vegetation Model. *Environmental Research Letters, 8*(3).https://doi-org.ludwig.lub.lu.se/10.1088/1748-9326/8/3/034023

Zhang, Z., Zimmermann, N. E., Stenke, A., Li, X., Hodson, E. L., Zhu, G., Huang, C., & Poulter, B. (2017). Emerging role of wetland methane emissions in driving 21st century climate change. *Proceedings of the National Academy of Sciences of the United States of America*, *114*(36), 9647–9652. 10.1073/pnas.1618765114

Appendix A

An analysis of the climatic controls was performed to quantify the importance of the climatic drivers that are responsible for modulating carbon fluxes. This was achieved by running multiple model simulations using single climate forcings, i.e., only temperature, only precipitation, and only CO_2, to identify which of the three variables influence the carbon dynamics the most and to identify possible differences between the sites. A linear regression analysis between the responses of net ecosystem productivity (NEP), CH_4, GPP, and R_{eco} to all forcings and single forcings were conducted and R^2 and RMSE were computed. The figure shows modelled gross primary production (GPP) for each peatland between 2006 and 2100 when forced only with projected atmospheric carbon dioxide content (yellow), temperature (red), precipitation (blue), as well as all three forcings combined (black). A moving average of 5 years has been applied to smoothen the data.

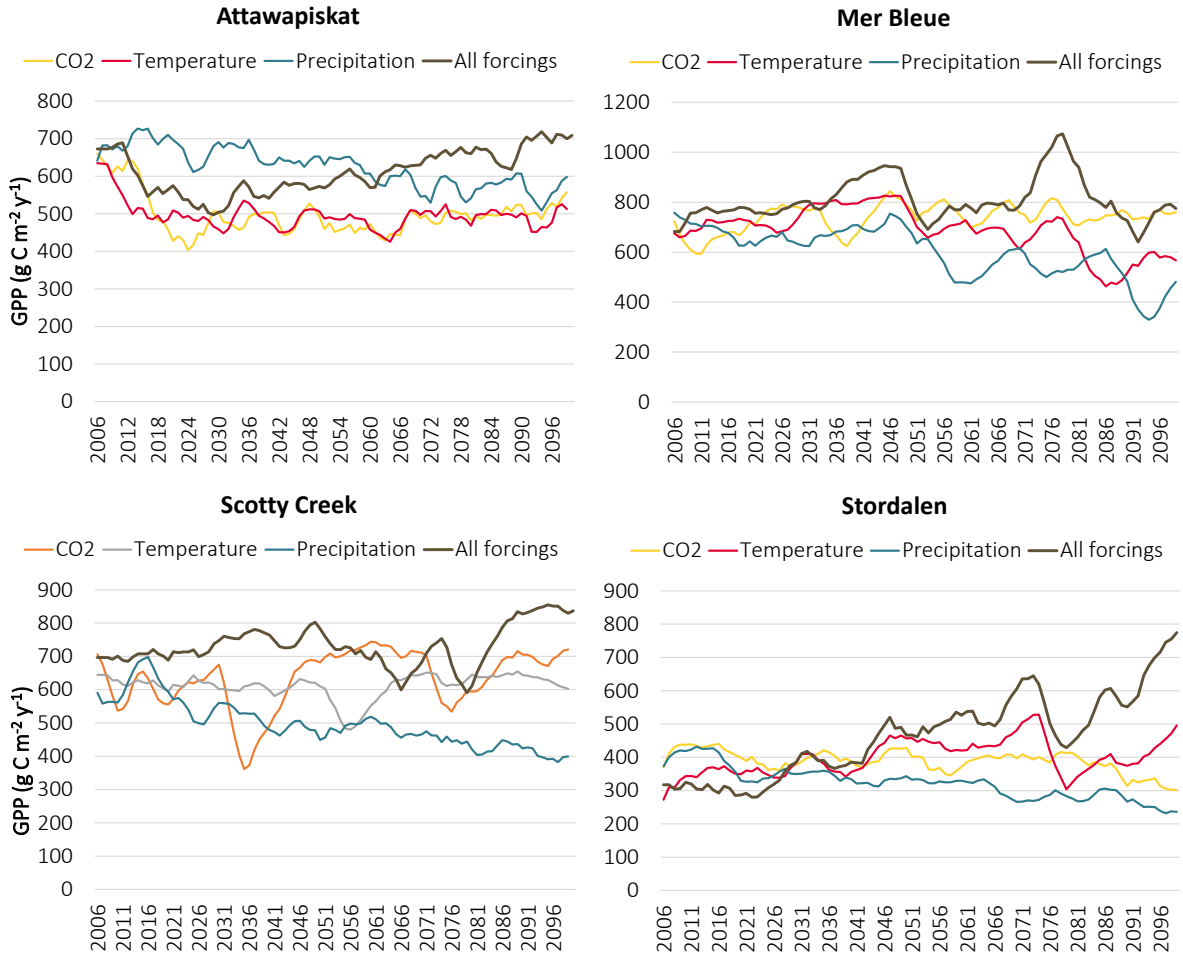

Appendix B

An analysis of the climatic controls was performed to quantify the importance of the climatic drivers that are responsible for modulating carbon fluxes. This was achieved by running multiple model simulations using single climate forcings, i.e., only temperature, only precipitation, and only CO_2, to identify which of the three variables influence the carbon dynamics the most and to identify possible differences between the sites. A linear regression analysis between the responses of net ecosystem productivity (NEP), CH_4, GPP, and R_{eco} to all forcings and single forcings were conducted and R^2 and RMSE were computed. The figure shows modelled ecosystem respiration (R_{eco}) between 2006 and 2100 when forced only with projected atmospheric carbon dioxide content (yellow), temperature (red), precipitation (blue), as well as all three forcings combined (black). A moving average of 5 years has been applied to smoothen the data.

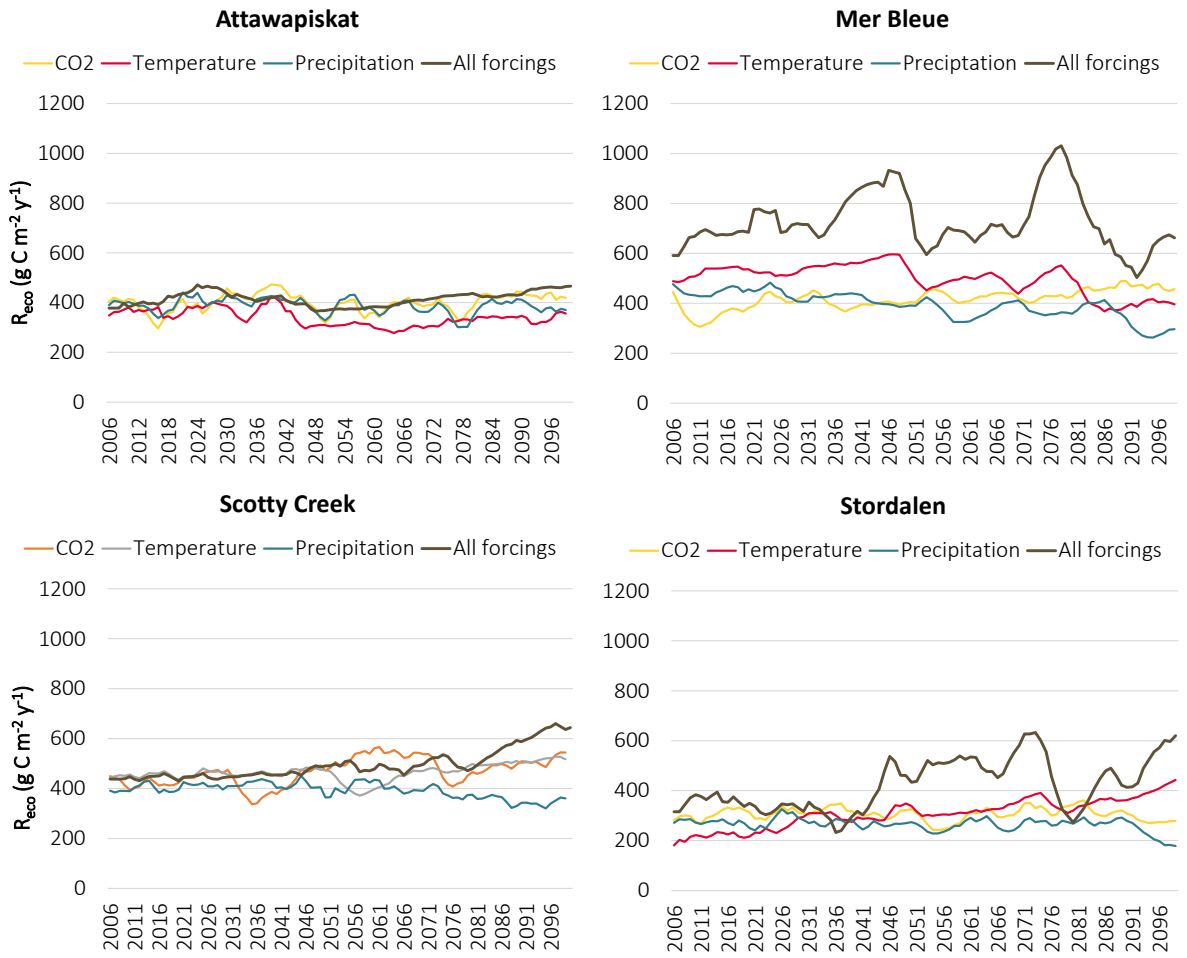

Appendix C

Statistics of the response of net ecosystem productivity (NEP), methane (CH_4) emissions, gross primary production (GPP), and ecosystem respiration (R_{eco}) to different climate forcings derived from a linear regression analysis between the standard experiment (all forcings) and the single forcing experiments (temperature, precipitation, or CO_2 concentrations) under RCP8.5. The statistics include the linear regression slope and R^2, as well as the RMSE. Each column (CO_2, temperature, precipitation) includes statistics from a linear regression analysis between the stated single forcing variable and the combined forcing scenario.

NEP	CO_2			Temperature			Precipitation		
	Slope	R^2	RMSE	Slope	R^2	RMSE	Slope	R^2	RMSE
Stordalen	1.4929	0.4464	52.48	1.3938	0.7963	31.83	1.0440	0.3948	54.87
Scotty Creek	0.1278	0.0125	40.41	0.4774	0.0742	39.13	-0.2991	0.0095	40.47
Attawapiskat	0.2231	0.0380	58.29	1.0473	0.8106	25.86	-0.1318	0.0078	59.19
Mer Bleue	0.3978	0.1193	36.29	0.3787	0.1225	36.22	0.1066	0.0175	38.32

CH_4	CO_2			Temperature			Precipitation		
	Slope	R^2	RMSE	Slope	R^2	RMSE	Slope	R^2	RMSE
Stordalen	0.8261	0.1805	27.6	1.0735	0.9719	5.1	0.5120	0.0804	29.3
Scotty Creek	0.2463	0.0736	5.76	1.2271	0.8633	2.2	0.2119	0.0719	5.76
Attawapiskat	0.4974	0.1139	14.9	1.1009	0.9193	4.5	-0.3338	0.0176	15.76
Mer Bleue	0.0973	0.0385	5.7	1.0199	0.8985	1.9	0.0429	0.0051	5.8

R_{eco}	CO_2			Temperature			Precipitation		
	Slope	R^2	RMSE	Slope	R^2	RMSE	Slope	R^2	RMSE
Stordalen	-1.5296	0.1465	94.15	1.1194	0.4201	77.60	-1.7638	0.2120	90.47
Scotty Creek	0.4758	0.2028	51.95	1.0848	0.3751	45.99	-1.4323	0.5498	39.04
Attawapiskat	0.3258	0.1373	30.19	0.5061	0.2690	27.79	0.1628	0.0216	32.15
Mer Bleue	-0.5429	0.0351	110.35	1.1168	0.3496	90.60	0.2729	0.0157	111.45

GPP	CO_2			Temperature			Precipitation		
	Slope	R^2	RMSE	Slope	R^2	RMSE	Slope	R^2	RMSE
Stordalen	-2.2873	0.3710	98.34	1.6981	0.5222	85.71	-2.0929	0.6722	70.99
Scotty Creek	0.0125	0.0003	60.25	0.0673	0.0016	60.21	-0.2490	0.0860	57.614
Attawapiskat	0.4278	0.1585	52.65	0.4419	0.0799	55.05	-0.6641	0.3702	45.55
Mer Bleue	0.3858	0.0566	84.73	0.3961	0.1668	79.63	0.0944	0.0119	86.71